Efficacy Appraisal of Synthetic Bimetallic Nano-aggregates for Fluoride Removal from Drinking Water through Batch and Fixed-Bed Column Operation Technology

Summary

By

Kankan Mukhopadhyay

DEPARTMENT OF GEOLOGY,

PRESIDENCY UNIVERSITY

Registration No. - R-14RS15210048

Supervisor:
Dr. Sasikumar Palani
Department of Chemistry
Presidency University
Kolkata 700073

Efficacy Appraisal of Synthetic Bimetallic Nano-aggregates for Fluoride Removal from Drinking Water through Batch and Fixed-Bed Column Operation Technology

Summary

By

Kankan Mukhopadhyay

DEPARTMENT OF GEOLOGY,

PRESIDENCY UNIVERSITY

Registration No. - R-14RS15210048

Supervisor:

Dr. Sasikumar Palani

1. Introduction

1.1. Problem Statement

For the last few decades, geo-environmental scientists at large are deeply alarmed by the growingly precarious threat allied with elevated level of fluoride in groundwater, causing 'Fluorosis' especially in countries like India, Bangladesh and Sri Lanka. Ironically, in 1937, groundwater contamination with fluoride was first detected in Nellore district of Andhra Pradesh, India (Shortt et al., 1937).Since then, fluorosis has been ubiquitously reported in at least 19 states of India(Saha et al., 2015) and 32 countries worldwide are also found to be endemic with fluorosis (Ayoob and Gupta, 2006). World Health Organisation, considering the annoying trend of fluoride poisoning in and around the world, fixed up optimum fluoride level in drinking water at 1.5 $mg.L^{-1}$, but diversified geological, climatological, and topographical pattern has aggravated the occurrence of fluoride in drinking water. Arid regions are prone to high fluoride concentration. Here, groundwater flow is slow and the reaction times with rocks are therefore long, thus leading to leaching of fluoride(Alagumuthu and Rajan, 2008; Chakrabarti and Bhattacharya, 2013).

1.2. Research Background

Defluoridation is the only practicable option to overcome the problem of excess fluoride in drinking water. Based on the nature of the mechanisms involved, defluoridation techniques can be generally grouped into coagulation, adsorption, ion exchange, electrochemical, and membrane processes. Ion-exchange can remove fluoride up to 90–95% but it is mostly dependent on the use of resins and the regeneration of resin is still a challenging issue. Adsorption is the most frequently used method for fluoride

removal. The criteria to select a suitable adsorbent include adsorption capacity, cost of the medium, ease of operation, potential for reuse, and possibility of regeneration.

In last decade, various metal oxide nanocomposites have been prepared and tried under simulating lab based conditions effectively as a fluoride scavenging media. Fluoride, due to its high electro-negativity and small ionic size, is classified as a hard base, which has natural strong affinity towards multivalent metal ions like Al(III), Fe(III), Zr(IV), Ce(IV), etc.(Ghosh et al., 2014; Wu et al., 2007). Among the various usable adsorbents, synthetic hydrous bi-metallic (Barathi et al., 2013; Biswas et al., 2009; L. Chen et al., 2016; P. Chen et al., 2016; Deng et al., 2011; Ghosh et al., 2014; Liu et al., 2010; Mukhopadhyay et al., 2017; Tang and Zhang, 2016; Tomar et al., 2013; Zhu et al., 2015) or poly metallic nano-crystallites (Biswas et al., 2010; Wu et al., 2007; Zhao et al., 2012) in various forms have emerged as potent defluoridation options over the years. Iron is selected as the base element in most of metal oxide mixture for its extreme natural abundance and excellent pollution scavenging property. Metals such as zirconium(Ghosh et al., 2014), cerium(Tang and Zhang, 2016), aluminium (Biswas et al., 2010), tin (Biswas et al., 2009), lanthanum (P. Chen et al., 2016), magnesium (Gao et al., 2014), manganese (Deng et al., 2011) are experimentally proven to possess strong affinity to form chemical linkage with fluoride. Therefore, combinations of iron with various metal oxides in varying proportions could be undertaken to increase the surface area and number of surface active sites. The differences in size and surface area of these diverse ions enhance adsorptive capacity. But except iron, aluminium, tin, most of these raw materials are very expensive that limits their applicability as nanoaggregates for environmental remediation. Thus use of iron nanoparticles to form nanoaggregates is considered for economic reasons for environmental clean ups. Again, improvement of adsorption capacity of these oxides by surface modification has also brought about

promising output and now most of the global research is swinging towards the deploying surface amended materials and their diversified application, particularly in water purification. In this context, Carbon, a versatile adsorbent and its various forms and their composites, is being increasingly explored by scientists across the world to upgrade them as surface modifier to enhance adsorption efficiency. As well as if recycling and scope of reuse of these adsorbents can be possible then cost of water treatment declined significantly.

1.3. Research Objectives

The aim of this research proposal to determine the fluoride ions removal behaviour from aqueous solutions and drinking water by crystalline nanoaggregates of [Fe (III)–Ce(IV)] named as CIHFO, prepared in the laboratory by Co-precipitation method considering both the adsorption kinetics and the isotherms to determine the adsorption rate and the maximum fluoride capacity of prepared material. The ultimate aspiration of this research proposal is to develop a cost effective nano-filtration medium to ensure domestic treatment and supply of fluoride free drinking water to poor population of West Bengal and global in general at the cheapest price. To achieve this goal, fixed–bed column operation, packed with CIHFO nanocomposite has been carried out in laboratory and design and fabrication of 'prototype' domestic filter unit has been done. Hence, the objectives of this research proposal are as follows:

I. Synthesis, characterization and application of novel nano-structured, non-toxic, bi-metallic oxide [Fe (III)–Ce (IV)] named as CIHFO for removal of fluoride from drinking water within range of 5-30 $mg.L^{-1}$ as reported to be present in groundwater in India.

II. To establish the applicability of newly developed CIHFO crystalline nanoaggregates for treatment of fluoride in household purpose, fixed-bed column operation to be accomplished.

III. Design and fabrication of a cost effective nano-filtration medium to ensure domestic treatment and supply of fluoride free drinking water at minimum price to poor community of West Bengal, in particular.

IV. Structural modification of CIHFO with graphene oxide and β–Cyclodextrin have been done with a goal to further enhancement of fluoride adsorption capacity of CIHFO.

2. Experimental Design

2.1. Preparation of Ce (IV)-incorporated hydrous Fe (III) oxide (CIHFO)

A Series of batch of cerium incorporated hydrous Fe (III) oxide were synthesised by co-precipitation method under ambient laboratory environment. The concentration of ferric chloride (0.1M) solution in 0.1M HCl was kept constant while the concentration of ammonium ceric nitrate in 0.1M HNO_3 was varied in different molar levels. Both solutions were mixed together and the pH of the mixture was increased to ~ 6.0-7.0 by drop wise addition of ammonia solution (mixture of 25% ammonia solution and 0.1 M ammonium carbonate solution). The brownish yellow gel like precipitate was developed and was left for aging for 24 hours. The precipitate was filtered through 0.45 μm membrane filter and repetitively washed with deionised water to remove extraneous contaminants. The residue was dried at 75°C (± 5°C) in an air oven. The hot mass immediately after drying was treated with cold water in order to break it into small particles. The air dried particles were ground, and sieved for collecting the particles of size between 50 and 100 mesh (particle size: 140-290 μm), and used for the conducting the batch experiments.

Hereafter an attempt has been made for enhancement of fluoride adsorption capacity, of CIHFO, the surface of newly developed CIHFO modified with both graphene oxide and β-Cyclodextrin (β-CD).

In case of column operation, agglomerated nanoparticles (size: 140-290 μm) of CIHFO was packed uniformly into the glass column (height: ~ 59 cm, internal diameter, id: 2.30 cm, cross sectional area: 4.153 cm^2) over glass wool followed by glass beads and cotton to avoid void spaces, channels and cracks in fixed-beds and set up to the desired bed heights. Before conducting experiment, each fixed- bed was washed five times with de-ionized water (pH: 7.0-7.5). The effluent of each column was collected fraction wise (250 mL) for fluoride analysis. The fluoride enriched solution (pH: 7.5±0.2, temperature: 30 ± 2º C) was allowed to flow down gravitationally through the fixed-bed columns.

3. Results and Discussion

3.1. Characterisation of Lab Bench Scale Prepared CIHFO, GO-CIHFO and βC-CIHFO

The powder X-ray diffraction (XRD), optical microscope (OM), scanning electron microscopy (SEM), transmission electron microscopy (TEM), atomic force microscopy (AFM), Brunauer–Emmett–Teller (BET) nitrogen (vapour) adsorption-desorption and Föurier transform infrared (FTIR) spectroscopy were used to characterize the materials (Instrumental details enclosed in Annexure –I)**.** Results obtained from instrumental analysis of Lab Bench Scale Prepared CIHFO and modified form of CIHFO to ensure the nanostructure orientation of proposed materials. XRD analysis of CIHFO shows amorphous nature of mixed metal oxide but after surface modification of CIHFO with GO and β Cyclodextrin, crystallinity of modified material confirm more structural stability of each nanocomposite. According

to Microscopic detailing, all three nanocomposites are mesoporic microcrystalline in nature with irregular surface morphology. BET analysis and FTIR analysis together provide information about surface area, pore volume, pore diameter and surface active groups present in all three materials respectively. Characterisation details of each synthesised material will be described in main thesis.

3.2. Batch and Column Operation

Batch and Column operations are mainly considered to determine the adsorption efficiency of any adsorbents in adsorption systems. Batch operations are usually executed to evaluate the ability of a material to adsorb as well as the adsorption capacity of the adsorbent. But the data obtained from batch operations are, in most cases, limited to a laboratory scale and hence could not be accurately applied in industrial and household systems. Column operations, on the other hand, provide information which could be profitable utilised in industries as well as household areas. Steps involved in batch and column adsorption study are elaborately described in Annexure – I.

3.2.1. Batch Adsorption Study

3.2.1.1. Influence of cerium content and calcination temperature in CIHFO on fluoride adsorption

Significant change in fluoride adsorption capacity has been noticed with changing of the Fe (III) to Ce (IV) mole ratio in CIHFO from 1.0: 0.0 to 0.0:1.0. Fluoride adsorption increased with enhancement of cerium content from 1.0:0.0 to 1.0:0.5, and declined there after till the Fe: Ce mole proportion changed to 1:1 (Fig.1A). Although, in this study, fluoride adsorption is highest for pure ceria material (25.3 $mg.g^{-1}$). But fluoride adsorption capacity is appreciably high compared to pure iron oxide when Fe: Ce = 1.0: 0.5. This might be beneficial when cost of proposed adsorbent is major concern.

Fig.1B shows the effect of calcination temperature upon the fluoride adsorption capacity ($mg.g^{-1}$) of calcined CIHFO. It was observed that fluoride adsorption capacity decreased consecutively with the increase of temperature at and above 300°C (573 K). Adsorbent, calcined at 200°C (473K) exhibited a maximum fluoride adsorption capacity (24.8 $mg.g^{-1}$) with initial fluoride concentration 15.0 $mg.L^{-1}$. CIHFO was prepared by simple co-precipitation method ensure formation of hydrous oxides of iron and cerium. Such surface active hydroxyl groups of metal oxides were presumably act as adsorption sites for fluoride adsorption. It is anticipated that, calcination temperature at 473K, hydrogen bonds the surface water molecules are break down which in turn exposed the surface hydroxyl groups to the solute for adsorption reaction, indicating higher adsorption value. With increase of calcined temperature (> 473 K), such hydroxyl groups are easily removed from the surface of metal oxides resulting in lower adsorption capacity of proposed adsorbent.

3.2.1.2. Influence of percentage of graphene oxide content in CIHFO on fluoride Adsorption

To evaluate the effect on fluoride adsorption capacity after doping of GO into the surface of CIHFO, a series of batch experiments have been conducted (Fig.1C). It was observed that with increase of weight percentage of GO up to 10%, fluoride adsorption capacity of GO-CIHFO has been increased in contrast to pure mixed metal oxide. After such percentage level of GO incorporation, no such noticeable increment in fluoride adsorption capacity observed. The main aim of this study is to develop a cost effective material as water purifier that can be applied in fluoride effected region of West Bengal (India) in affordable price. To achieve this goal, 10% GO-CIHFO is selected for rest of the experimental studies.

3.2.1.3. Effect of Beta Cyclodextrin Molar concentration variation on fluoride uptake capacity of βC-CIHFO

It was observed that with increase in molar concentration of Beta Cyclodextrin in both solution pH 3.0 and pH 7.0, fluoride adsorption capacity of βC-CIHFO improved up to 0.04 M concentration of Beta Cyclodextrin then declined (Fig.1D). Hence, 0.04 M Beta Cyclodextrin optimised for the formation of βC-CIHFO nanocomposite.

The main aim of this study is to develop a cost effective material as water purifier that can be applied in fluoride effected region of West Bengal (India) in affordable price. To achieve this goal, 10% GO incorporated CIHFO (GO-CIHFO) and 0.04M Beta Cyclodextrin encapsulated CIHFO (βC-CIHFO) are selected for rest of the experimental studies.

3.2.1.4.Effect of Adsorbent dose

To determine the effect of adsorbent dose on fluoride removal, adsorbent dose was varied from 0.05 to 2.0 g CIHFO per 50 mL fluoride solution of (C_i = 10.0, 15.0 and 20.0 $mg.L^{-1}$); 0.01 g to 1.0 g GO-CIHFO nanocomposite in 50 mL of fluoride solution (C_i =10 and 15 mg. L^{-1}) and 0.01 g to 1.0 g βC-CIHFO nanocomposite in 50 mL of fluoride solution (C_i = 20 mg. L^{-1}) for adsorption reaction at 30°C (303 K) and at pH_i ~ 7.0. It has been noticed that the fluoride removal capacity (Q_e, $mg.g^{-1}$) declined for a given C_i value with the increase of adsorbent dose (Fig.2). This phenomenon can be well elucidated by the surface sites heterogeneity model. As per this model, any surface sites are composed of a series of spectrum of binding energies. When dose applied in minute quantity, then availability of exposed surface sites enhanced the adsorption capacity (Q_e) value. Reversible condition will set on with rise of adsorbent dose, which

is similar with other researchers(Biswas et al., 2009; Mukhopadhyay et al., 2017; Saha et al., 2015).

3.2.1.5. Effect of pH upon Fluoride adsorption capacity of CIHFO, GO-CIHFO and βC-CIHFO

Initial solution pH and pH_{ZPC} of any adsorbent are considered as two important factors that play a crucial role in any adsorption mechanism of adsorbate over adsorbent. Adsorption of any anion is influenced by the presence of hydroxyl ions in solution. To apprehend fluoride adsorption over all these three adsorbent, a set of experiments were carried out in the pH range 3-10, in room temperature. The pH_{ZPC} of CIHFO, GO-CIHFO and βC-CIHFO was found to be (5.2,±0.2), (6.2,±2) and (6.4,±0.2) respectively, depicting that the adsorbent surface is positive below pH_{ZPC} and negative above pH_{ZPC}. Fig. 3(A-C) and Fig. 3(D-F) represents pictorial explanation of the effect of pH on fluoride adsorption capacity of three adsorbents and pH_{ZPC} of adsorbents as well. It was observed from experimental results that maximum equilibrium adsorption capacity obtained at pH 3.0 for all fluoride concentrations. Moreover, the fluoride adsorption capacity of all adsorbents reduced drastically at pH > 7. Such declining trend of fluoride uptake capacity can be justified by the fact that with increasing pH the adsorbent retains a negative surface charge ($pH > pH_{zpc}$), that lean towards columbic repulsion for negatively charged fluoride ions. Concentration of hydroxyl ions (OH^-) also increase at basic pH range that also competed with the fluoride for the active binding sites of the adsorbent (Barathi et al., 2014; Mohan et al., 2016; Mukhopadhyay et al., 2017).

As per HSAB principle, Fe^{3+} and Ce^{4+} are act as hard acid. Hard acids prefer binding to the hard bases to give ionic complexes. In aqueous medium, Fe^{3+} and Ce^{4+} could be present as cationic hydroxide forms and could easily interact with fluoride ions by

electrostatic attraction. When solution pH is in acidic range, adsorption occurs by electrostatic interaction;

$$M\text{-}OH + F^- \rightarrow M\text{-}F + OH^- \ (M\text{-}Fe^{3+}, Ce^{4+}) \quad (pH < pH_{ZPC}) \qquad [R_1]$$

At basic solution pH range, protonation of surface occurs. In such condition, adsorbent surface is to be negative and imparts Coulombic repulsion on fluoride ion. This can be demonstrated by R_2.

$$M\text{-}OH + F^- + OH^- \rightarrow M\text{-}O^- + F^- + OH_2 \ (M\text{-}Fe^{3+}, Ce^{4+}) \ (pH > pH_{ZPC}) \qquad [R_2]$$

Fluoride adsorption over each adsorbent hence can be happened by Ligand/anion exchange or by hydrogen bonding;

$$M\text{-}OH_2^+ + F^- \rightarrow M\text{-}F + H_2O \quad (M\text{-}Fe^{3+}, Ce^{4+}) \qquad [R_3]$$

$$O\text{-}H + F^- \rightarrow O\text{-}H\cdots F^- \qquad [R_4]$$

Finally, it can be concluded that Fluoride adsorption over each adsorbent individually is a combination of hydrogen bonding, electrostatic interaction and also involved ligand exchange in between hydroxyl groups and fluoride ions (Mohan et al., 2016).

3.2.1.6. Effect of Contact Time on Adsorption Process and Kinetic Modelling

The effect of contact time with variation of both initial fluoride concentration and temperature upon fluoride uptake capacity of proposed three adsorbents was studied sequentially to comprehend the pattern of adsorption mechanism of ongoing adsorption process. Primarily, rate of adsorption is vastly influenced by the available free active binding sites of proposed adsorbent and high concentration gradient of fluoride. It was observed that in all experimental adsorption set up, saturation time (equilibrium time) is highly independent of initial concentration (C_i) of fluoride solution. The fluoride

uptake was found to be in rising trend with increase of initial fluoride concentration until the equilibrium time was achieved.

Time-rate adsorption of proposed adsorbent, on fluoride uptake at different temperature(288K or 293K, 303K and 313K) with fixed fluoride solution (15 or 10 $mg.L^{-1}$) also revealed that period of saturation remains unchanged irrespective of the rise of temperature in each adsorption study thus is independent of temperature variation also.

In this study, various mathematical expressions of kinetic models such as Pseudo-first order and pseudo-second-order kinetics models, Mass transfer Study, Intra-particles diffusion model, Elovich model, Richenberg Model have been applied to explore the rate controlling step and actual adsorption mechanism of fluoride by proposed adsorbent involved in present process.

3.2.1.6.1. Pseudo-first order and pseudo-second-order kinetics models

Kinetic data of present study were analysed by most universally used non-linear form of pseudo-first order (Eq.5) and pseudo-second order (Eq.6) model equations (Annexure-I). The non-linear plots of the kinetic data by pseudo-second order model and pseudo-first order model fitting are shown in Fig.4 and Fig.5 respectively.

Inspection of the data revealed that more than 80% of the loaded fluoride transferred to the material surface from the solution in time t = 0 to 40 minutes, and rest 15-20% of the fluoride in solution needed longer time to transfer on the solid surface. The later slow solute transfer may be due to the Coulombic and physical hindrance of fluoride already hosted over the solid surface from solution as well as decrease of the available solute concentration and adsorption sites of the adsorbent. Considering the values of regression coefficient (R^2) and statistical error chi-square (χ^2), it can be said that the

fluoride adsorption over CIHFO surfaces has occurred almost in accordance to both pseudo-first and pseudo-second order models. The $Q_{t(exp)}$ values were found too close to the modelled Q_t value from pseudo-second order kinetics model at any particular time and temperature. It can be assumed from such results that fluoride adsorption process can be well fitted with pseudo second order model hence the adsorption process followed chemisorption.

Increase of the rate of the reaction with temperature is associated with the availability of more fractions of adsorbent species with threshold energy, required for the effective molecular collision.(Saha et al., 2015). It is observed that that the value of Q_t, in case of CIHFO decreased with increase of temperature of the reactions. Decrease of the value of Q_t value with increasing temperature designates the exothermic nature of adsorption reaction. In the case of increasing C_i, the rate change showed similarity with the previous but the value of Q_t inclined with the value of C_i. This is presumably due to the increase of availability of solute loading per unit of active sites.

In case of GO-CIHFO and βC-CIHFO, The parameters of the kinetic model equations (5) and (6) as estimated from the plots are demonstrated in Table-1 and Table-2. Emphasizing on the values of regression coefficient (R^2), it can be said that the fluoride adsorption over both GO-CIHFO and βC-CIHFO surfaces has occurred almost in accordance of pseudo-second order model. The $Q_{t(exp)}$ values were found too close to the modelled Q_t value from pseudo-second order kinetics model at any particular time and temperature. The chemisorption is one of the controlling factors of any adsorption kinetics is expressed by pseudo second order model. Hence, it can be assumed from such results that as fluoride adsorption process was well fitted with pseudo second order model then adsorption process might be following chemisorption (Biswas et al., 2009; Mohan et al., 2016; Mukhopadhyay et al., 2017).

3.2.1.6.2. Mass transfer Study

Fig.6 presents the Mckay *et al.* model plot for the mass transfer of fluoride for all three proposed adsorbents. The plot of good linear fitting with the experimental data denoted that the external mass transfer step was present during the adsorption process. The mass transfer coefficients (β_1) for the diffusion of fluoride from liquid film boundary to the surface of adsorbent have been determined by the slopes of the plots of ln [$C_t/C_i - 1/(1 + mk)$] vs. t (min) at different temperature (288K or 293K, 303K and 313K) with fixed fluoride concentration (15 $mg.L^{-1}$ for GO-CIHFO and βC-CIHFO and 10 $mg.L^{-1}$ for CIHFO) with solution pH 7.0 are shown in Fig.6 and values are given in Table-4. All the values of mass transfer coefficient are act as an indication of sufficiently rapid transfer of adsorbate species from bulk to the surface or interface in neutral pH.

3.2.1.6.3. Intra particles diffusion model

The plot of Q_t vs. $t^{0.5}$ (min) shown in Fig.7 and Fig.8 signify the corresponding Weber–Morris model to evaluate the prospect of intraparticle diffusion on the adsorption process of fluoride onto CIHFO, GO-CIHFO and βC-CIHFO. The plots were found to be significantly linear with high value of R^2, and K_{id} values have been determined by their respective slopes at varied experimental conditions (Table-1 and Table-2). If the plot of Q_t vs. $t^{0.5}$ is a straight line and passes through the origin, then the intraparticle diffusion is thought to be as the rate controlling step (Biswas et al., 2009; Ranjan et al., 2009).In this adsorption system, although these plots are linear they did not pass through origin, which indicated that the intraparticle diffusion was not the sole rate controlling step. Hence, it can be assumed that fluoride adsorption over proposed adsorbent occurred via a complex mechanism involving both external mass transfer and intraparticle diffusion as the rate determining step. This observation was further

strengthened by the value of the intraparticle diffusion coefficient (D), which can be calculated by the following equation.

$$D = \frac{0.03r^2}{t^{0.5}} \quad \text{(Eq.1)}$$

Here, r (cm) represents for the average radius of the adsorbent particle and $t^{0.5}$ (min) is the time required for half of the adsorption. If the D value is in the range of 10^{-11} (cm^2 s^{-1}) then intraparticle diffusion is the only rate determining step. In the present adsorption system, the value of D obtained as (7.46×10^{-8} cm^2 s^{-1}) was in the order of 10^{-8}, designating that intraparticle diffusion was not the only rate controlling step.

3.2.1.6.4. Elovich model

Elovich model is another widely accepted kinetic model used successfully to describe second order kinetics with a postulation that solid surface of adsorbent are energetically heterogeneous. It has been broadly accepted that chemisorption process can be elucidated by its linear form of semi-empirical equation (Eq.10; Annexure-I).The Elovich coefficients have been assumed from the plots Q_t versus ln (t)(min). The initial adsorption rate, a, and desorption constant, b, were calculated from the slope and intercept of the straight-line plots and values obtained from plots have been tabularized in Table-1 and Table-2. It has been observed that applicability of the simple Elovich equation for the present kinetic data indicates that the Elovich equation was able to describe properly the kinetics of fluoride adsorption on CIHFO, GO-CIHFO and βC-CIHFO (Fig.9&10). The value of a and b varied as a function of both solution concentration and solution temperature. Good correlation coefficient (R^2) for both concentration variation and temperature variation implied that adsorption kinetics followed by pseudo-second order kinetic model based on assumption that

chemisorption may be the rate determining step involving ion exchange in between adsorbent and adsorbate (Ranjan et al., 2009).

3.2.1.6.5. Richenberg Model

Fig.11 and Fig.12 present the plots of the Richenberg model [β_t vs. t (min)] for CIHFO, CIHFO and βC-CIHFO respectively at different solution concentration and at different temperature in neutral pH. The plots with good linearity accompanied with high correlation coefficient (R^2) values (given in Table-1 and Table-2) and did not pass through origin. These results is indicative of the fact that intraparticle diffusion is not the only rate controlling step and this is also support the results obtained from intraparticle diffusion model.

The factor β_t was calculated from the slope and used to calculate the effective D_i and both are recorded in Table-1 and Table-2. If the by values of D_i have been ranged in between of 10^{-6} to 10^{-8} cm^2 s^{-1}, the rate determining step dominated external mass transfer. Whereas the values of D_i when obtained in the range of 10^{-11} to 10^{-13} cm^2s^{-1}, intraparticle diffusion is considered as rate controlling step. From the Table-1 and Table-2, it has been observed that the values of D_i for the adsorption of fluoride on each adsorbent was in the order of 10^{-6} cm^2 s^{-1},Which is more than 10^{-11} cm^2 s^{-1}, then, intraparticle diffusion was not the only rate controlling step, external mass transfer was also involved in adsorption process. Values of film diffusion (D_1) and pore diffusion (D_2) were assessed and mentioned in Table-1 and Table-2. Negative exponential values with same order of magnitude assure that both film and pore diffusion process involved in adsorption mechanism [37].

3.2.1.7. Equilibrium Analysis

To recognise the adsorption feasibility of a newly developed adsorbent, different adsorption isotherm models were applied for better understanding of the adsorption process. Langmuir and Freundlich and D-R isotherm are most convenient fundamental isotherm models that can be applied to illustrating the surface properties and adsorption mechanism. For adsorption isotherm study, experiments were carried out at four different temperatures 288K (293K for CIHFO), 303K, 313K and 323 K with initial fluoride concentration in a range of 5 to 60 $mg.L^{-1}$, with solution pH 7.0 and with adsorbent dose 0.2 $g.L^{-1}$ for GO-CIHFO and βC-CIHFO and 0.5 $g.L^{-1}$ for CIHFO respectively.

3.2.1.7.1. Langmuir Isotherm

The Langmuir isotherm constants; Q_m (the maximum monolayer adsorption capacity,$mg.g^{-1}$) and K_L (the equilibrium constant related to net enthalpy change of the reaction, $L.mg^{-1}$) respectively were obtained from the plot of non-linear form of Langmuir equation (Eq. 17) with the help of origin software spread sheet are presented in Table-3 and in Fig.13. The Langmuir uptake capacity of CIHFO, GO-CIHFO and βC-CIHFO were found 22.55 $mg.g^{-1}$, 80.42 $mg.g^{-1}$ and 52.32 $mg.g^{-1}$ at neutral pH and at 303 K (30°C). The increasing trend of Q_m value for both adsorbent GO-CIHFO and βC-CIHFO with higher temperature range indicated the endothermic nature of adsorption process while decreasing Q_m value of CIHFO with increasing temperature support exothermic nature of adsorption process.

3.2.1.7.2. Freundlich Isotherm

The values of regression coefficient (R^2), and Freundlich constant (n and K_F) obtained from non-linear Freundlich isotherm equation (Eq. 18) analysis are given in Table-3

and in Fig.13. Based on values of regression coefficient (R^2), it can be easily concluded that the fitting of equilibrium data were much better with the Freundlich model rather than the Langmuir model. From the assessed values of n, it was perceived that degree of Freundlich coefficient (1/n) is laid in between 0 and 1 that is assuring favourable adsorption of fluoride upon all three prepared proposed adsorbents. Values of K_F (Freundlich adsorption capacity) was obtained at temperature 303K for solution pH 7.0 for CIHFO, GO-CIHFO and βC-CIHFO were 10.88, 4.71 and 8.30 ($mg.g^{-1}$) respectively.there was no such brisk enhancement in K_F (Freundlich adsorption capacity) values in higher temperature zone in neutral pH. Therefore, 303K and solution pH 7.0 can be considered as optimised temperature and pH for adsorption of fluoride for all three adsorbents.

3.2.1.7.3. D-R Isotherm

Evaluation of the free energy of reaction of any adsorption process and to envisage the nature of adsorption, whether physical, ion-exchange or chemical, D-R isotherm is most widely accepted model in this field. To obtain D–R isotherm parameters, ln Q_e vs. E^2 were plotted and found to be significantly linear at all the temperatures (Fig.14).The parameters of this isotherm, such as energy of adsorption E_{DR} ($kJ\ mol^{-1}$), β ($mol^2\ kJ^{-2}$) and R^2, are mentioned in Table-3. The substantially high value of R^2 associated with applied temperatures suggested the applicability of the D–R isotherm. D-R equation and according to value of E_{DR}, an adsorption process can be categorised in three types such as (i) physisorption if E_{DR} = 8.0 kJ mol^{-1}, (ii) ion-exchange if E_{DR} = 8.0–16.0 kJ mol^{-1} and (iii) chemisorption if ED–R > 16.0 kJ mol^{-1}(Ghosh et al., 2014; Mukhopadhyay et al., 2017)

For CIHFO, gradual increase of the E_{DR} value noticed with rise of temperature from 12.61 to 20.32 kJ mol^{-1} indicates the adsorption of fluoride occurring via ion-exchange

to chemisorption phenomena. At 303K the E_{DR} obtained for present case is 15.50 kJ mol^{-1} indicated to be at borderline of ion-exchange and chemisorption.

E_{DR} values of GO-CIHFO established from D-R isotherm were ranged in between 8.32-9.87 with fluoride solution pH 7.0 indicates the adsorption of fluoride shows predominant trait of phsisorption inclined to ion-Exchange phenomena. At 303K temperature, 9.13 kJ mol^{-1} strongly emphasized on ion-exchange phenomenon.

E_{DR} values of βC-CIHFO obtained from D-R isotherm were ranged in between **10.17-8.77** with fluoride solution pH was 7.0 specifies that the adsorption of fluoride over βC-CIHFO strongly follow ion-Exchange phenomena. At 303K temperature, **9.95** kJ mol^{-1} ideal example of D-R value that supports ion-exchange phenomenon.

3.2.1.8.Thermodynamics Studies

The plot of ln K_C vs. 1/T (Van't Hoff Plot) for fluoride adsorption for all three adsorbents in solution pH 7.0 are shown in Fig.15.The thermodynamic parameters (ΔG°, ΔH°, ΔS°) thus calculated are updated in Table-4. The negative values of ΔG° specified the spontaneous nature of adsorption process. Hence adsorptive forces required for reaction are fairly strong enough to overcome the potential barrier and greater negative values of ΔG° associated with rise of temperature indicated that higher temperature favours adsorption process. The highly negative value of ΔH° (-36.279 kJ mol^{-1}) for CIHFO indicates that the adsorption process is also exothermic in nature. This was in agreement with the results of the isotherm analysis. The entropy change (ΔS°) was found to be (-86.537 J mol^{-1} K^{-1}), indicating the irreversibility and stability of the adsorption process.

Positive values of enthalpy (ΔH°) for both GO-CIHFO and βC-CIHFO suggested the endothermic nature of adsorption process. The positive values of ΔS° for both GO-

CIHFO and βC-CIHFO conditions of whole adsorption experiment system, recommended high degree of freedom of solute molecules owing to adsorption, thus randomness was increased during the adsorption process. This was presumably due to desorption process that simultaneously took place during adsorption, increased the entropy (ΔS°) at the solid–liquid interface(Saha et al., 2016).

3.2.1.9.Activation Energy

The plot of ln k_2 against 1/T, a straight-line with slope (-E_a/R) was obtained (Fig.15). The magnitude of activation energy (E_a) for adsorption of fluoride on the surface of adsorbent has been evaluated from slope of the plot. It was 26.07 KJ mol^{-1}, 22.61 KJ mol^{-1} and 27.10 KJ mol^{-1} respectively for adsorbent CIHFO, GO-CIHFO and βC-CIHFO respectively. Magnitude of E_a is lesser than 42 KJ mol^{-1},then diffusion control process is thought to be accompanying the adsorption process(Podder and Majumder, 2016). E_a value higher than 42 KJ mol^{-1} is envisaged chemically controlled reaction process also occurred. Here, high magnitude of activation energy for this adsorption study implies that fluoride has high combining affinity with proposed adsorbent surface as diffusion process prefers the movement of solute to the external surface of adsorbent. Considering the value of E_a, it can be assumed fluoride adsorption upon the surface of proposed material is supposed to be associated with ion-exchange that is also significantly support the adsorption pattern obtained from D-R isotherm study.

3.2.1.10. Effect of co-occurring ions on Fluoride adsorption

Groundwater resource contains a wide range of anions such as SO_4^{2-}, HCO_3^-, HPO_4^{2-} etc. in addition with F^- which may have affinity towards same active sites on adsorbent as reported earlier(Biswas et al., 2010; Mukhopadhyay et al., 2017; Wen et al., 2015).A series of experiments were carried out in presence of these anions with different

concentration to explore their influence upon fluoride uptake capacity. In adsorbent CIHFO, sulphate ions hinder fluoride adsorption effectively. It was observed that as the sulphate concentration increased from10.0 to 150 $mg.L^{-1}$, the fluoride adsorption amount (9.5 $mg.g^{-1}$) decreased to 3.3 ($mg.g^{-1}$), which is only ~30% of the initial value. However in presence of other ions there was no such change occurred in fluoride adsorption capacity. Hence, the sequence of the adverse influence of the tested ions on fluoride adsorption over CIHFO can be given as SO_4^{2-}>HCO_3^-> HPO_4^{2-}>NO_3^-> Cl^-.In case of GO-CIHFO, It was observed that these anions at altered concentrations impose no such adverse effects upon fluoride removal even at high concentration. It presumably occurs due to weak or lack of interaction in between adsorbent active sites and said anions. In case of βC-CIHFO, It was observed that as the sulphate concentration increased from 10.0 to 150 ($mg.L^{-1}$), the fluoride adsorption capacity 18.21 ($mg.g^{-1}$) decreased to 11.14 ($mg.g^{-1}$) and increase of phosphate concentration from 0.1 to 10 ($mg.L^{-1}$) resulted significant change in fluoride adsorption from 18.94 ($mg.L^{-1}$) to 13.87 ($mg.L^{-1}$).Categorisation of co-occurring ions on fluoride adsorption can be sequenced as SO_4^{2-}> HPO_4^{2-}> HCO_3^->NO_3^-> Cl^-. Other ions produced so such adverse impact upon fluoride adsorption.

3.2.1.11. Desorption and Re-usability of Proposed Adsorbent

Regeneration is a useful tool to regain the adsorptive capacity of any adsorbent. Development of a cost-effective adsorbent and commercialisation of it, is highly dependent on the recycling nature of the adsorbent. To establish the reusability of proposed material desorption study was carried out. For fulfilling the experimental study purpose, fluoride adsorbed GO-CIHFO and βC-CIHFO are generated by adsorbing 60 $mg.L^{-1}$ fluoride solution in 10 $g.L^{-1}$ of GO-CIHFO and βC-CIHFO respectively at pH 7.0.Then Fluoride adsorbed materials were subjected to desorption

study by maintaining pH values (8-13) by addition of 0.1 M NaOH or 0.1 M HCL solution as per requirement. The fluoride free material then air dried and collected for repeating the aforesaid adsorption-desorption study (Barathi et al., 2014; Mohan et al., 2016). The adsorbents were reused for five cycles in this study. It was experimentally approved that no such rise in fluoride concentration was noticed in solution up to pH 9 for both adsorbent, afterward desorption efficiency of fluoride sequentially increased to 73.77 % for GO-CIHFO and 75.19 % for βC-CIHFO at pH 13. During recycling, in case of GO-CIHFO, the percentage of adsorption of fluoride was found to be 69.19%, and 16.66% respectively for the 1st and 5th cycles of reuse. For βC-CIHFO, the percentage of adsorption of fluoride was found to be 71.11%, and 21.02% respectively for the 1st and 5th cycles of reuse (Mohan et al., 2016).

The Desorption percentage for CIHFO improved with increasing basicity and maximum 61% desorption occurred. As the process is predicted as borderline chemisorption and exothermic in nature so it is quite obvious the product is gaining more stability than the reactant. And as the desorption tendency is moderate so the leaching tendency of fluoride to the environment also less.

3.2.1.12. Removal of Fluoride from a Natural Groundwater Sample

Purulia District situated in the eastern fringe of State of West Bengal, India, is now in limelight for high concentration of Fluoride in Groundwater and situation is get worse day to day. Considering such adverse situation of this region, water samples have been collected from few selective hand pump attached tube-wells of Kashipur block of Raghunathpur Subdivision of Purulia District. Water sample collected from (Latitude - 23°28’303" N; Longitude- 86° 40’027" E, Elevation-161m) Kharai village of Kashipur block of Purulia district, West Bengal, was reported with high fluoride concentration (9.05 $mg.L^{-1}$), among all collected samples. Some physic-chemical parameters such as

pH (7.36), iron (total) (0.77 mg.L^{-1}), calcium (18.05 mg L^{-1}), magnesium (3.69 mg.L^{-1}), hardness (21.74 mg.L^{-1}), TDS (679 mg.L^{-1}), salinity (473 mg.L^{-1}), conductivity (959 μS) and turbidity (18 NTU) were also carried out to evaluate overall water quality. One litre of this water sample was stirred (500 rpm) with the help of magnetic stirrer for 2 hours with changing dosage for each adsorbent namely, CIHFO, GO-CIHFO and βC-CIHFO from 0.1 g to 1.5 g. After completion of the experiment time, treated water was filtered and analysed for the fluoride level. It was found that fluoride level reduced from 9.05 mg.L^{-1} to below 1.0 mg.L^{-1} when the dosage of CIHFO-2.4 g.L^{-1}; dosage of GO-CIHFO - 1.2 g.L^{-1} and dosage of βC-CIHFO- 1.8 g.L^{-1} respectively employed. Thus, it can be experimentally approved that 2.4 g of CIHFO, 1.2 g of GO-CIHFO and 1.8 g of βC-CIHFO can efficiently reduce fluoride level to desired concentration (1.0 mg.L^{-1}) which is well below the WHO recommended guide line for maximum fluoride concentration level(Mukhopadhyay et al., 2017).

3.3. Fixed Bed Column Operation for Removal of Fluoride

Three most important parameters considered during column operation for breakthrough curve analysis, were bed depth, effluent discharge rate (Fig.16) and fluoride concentration variation (C_i, mg.L^{-1}) in feed water. Noticeable enhancement in effluent volume (V_b) was observed at breakthrough point (Fig. 16A) (fluoride concentration at C_b: 1.5 mg. L^{-1}) with increase of bed depth (6.0, 10.0 and 14.0 cm) or empty bed contact time (EBCT- 24.90, 41.52 and 58.13 min, respectively). Apparently such enrichment was not proportionate enough might be due to the increase of mass transfer resistance into the inner surface of the particles packed in fixed beds. Solution feeding rate also inversely proportionate with breakthrough points. At slow solution feeding rate, interaction time with adsorbent was high enough resulting in delayed appearance of breakthrough points (higher V_b) (Fig.16B). Effect of change in initial fluoride

concentration on fixed–bed (10 cm) column operation was pictorially represented in Fig.17C. Change of initial fluoride concentration (C_i mg. L^{-1}) in feed samples with fixed solution flow rate (1mL.min^{-1}) revealed that the breakthrough point achieved earlier resulting lower breakthrough volume with increasing fluoride concentration causing huge solute load at per unit area of the surface of the fixed beds, resulting in fast exhaustion of fluoride removal capacity of CIHFO packed fixed-beds. The effluent collected from the CIHFO packed fixed-bed (10 cm) column with 1mL.min^{-1} solution flow rate with initial fluoride concentration(C_i - 5.0 mg.L^{-1}) at breakthrough point (C_b -1.5 mg.L^{-1}) and some preliminary water quality parameters such as pH (6.7), iron (total) (4.8 mg.L^{-1}), calcium (65.09 mg L^{-1}), magnesium (36.43 mg.L^{-1}), hardness (101.52 mg.L^{-1}), TDS (892 mg.L^{-1}), salinity (449 mg.L^{-1}), conductivity (750 µS) and turbidity (42 NTU) carried out to assess overall water quality of treated water. It was observed that the present fixed bed column efficiently reduced concentration of fluoride to its permissible level. The quality of treated water ensured that the CIHFO packed column could be applicable efficiently for continuous removal of fluoride from the contaminated water.

Conclusion

↔ Hydrous cerium (IV)-incorporated iron (III) oxide (CIHFO) is highly porous microcrystalline and amorphous material with high surface area relative to the iron (III) oxide. CIHFO itself and after surface modification (with GO and β–Cyclodextrin) both the adsorbents exhibit micro crystalline particles of nano-dimension with irregular surface morphology.

↔ For fluoride adsorption, these three adsorbents (CIHFO, GO-CIHFO and βC-CIHFO) significantly show that surface reaction occurs according to the pseudo-first as well as pseudo-second order kinetics with boundary layer (film) diffusion process.

↔ The better adherence of the equilibrium data with the Freundlich isotherm suggests the surface heterogeneity of CIHFO multilayer adsorption phenomenon. The change of enthalpy (ΔH°), Calculated E_{DR} value and magnitude of activation energy also favoured these results.

↔ It was observed that minute amount of all the proposed adsorbents can treat high fluoride containing (9.05 $mg.L^{-1}$) groundwater and reduce contamination level below permissible level successfully. Application of proposed material in column operation can not only suggest its usability for groundwater treatment in lab-bench scale level only, but it can be also be used as purifier medium packed in domestic filter units.

Acknowledgement

Tthis research work was carried out from the fund sanctioned by the Department of Science and Technology (DST), Govt. of India herein the form of a Woman Scientist-B, (DST/Disha/SoRF-PM/064/2013/C dated 14/09/2015).

References:

1. Alagumuthu, G., Rajan, M., 2008. MONITORING OF FLUORIDE CONCENTRATION IN GROUND WATER OF KADAYAM BLOCK OF TIRUNELVELI DISTRICT, INDIA: CORRELATION WITH PHYSICO-CHEMICAL PARAMETERS. RJC Rasayan J. Chem 1, 920–928.
2. Ayoob, S., Gupta, A.K., 2006. Fluoride in drinking water: A review on the status and stress effects. Crit. Rev. Environ. Sci. Technol. https://doi.org/10.1080/10643380600678112
3. Banerjee, S., Chattopadhyaya, M.C., 2017. Adsorption characteristics for the removal of a toxic dye, tartrazine from aqueous solutions by a low cost agricultural by-product. Arab. J. Chem. https://doi.org/10.1016/j.arabjc.2013.06.005
4. Barathi, M., Krishna Kumar, A.S., Kumar, C.U., Rajesh, N., 2014. Graphene oxide-aluminium oxyhydroxide interaction and its application for the effective adsorption of fluoride. RSC Adv. https://doi.org/10.1039/c4ra10006a
5. Barathi, M., Santhana Krishna Kumar, A., Rajesh, N., 2013. Efficacy of novel Al-Zr impregnated cellulose adsorbent prepared using microwave irradiation for the facile defluoridation of water. J. Environ. Chem. Eng. https://doi.org/10.1016/j.jece.2013.09.026
6. Biswas, K., Gupta, K., Ghosh, U.C., 2009. Adsorption of fluoride by hydrous iron(III)-tin(IV) bimetal mixed oxide from the aqueous solutions. Chem. Eng. J. https://doi.org/10.1016/j.cej.2008.09.047
7. Biswas, K., Gupta, K., Goswami, A., Ghosh, U.C., 2010. Fluoride removal efficiency

from aqueous solution by synthetic iron(III)-aluminum(III)-chromium(III) ternary mixed oxide. Desalination. https://doi.org/10.1016/j.desal.2010.01.019
8. Chakrabarti, S., Bhattacharya, H.N., 2013. Inferring the hydro-geochemistry of fluoride contamination in Bankura district, West Bengal: A case study. J. Geol. Soc. India. https://doi.org/10.1007/s12594-013-0165-9
9. Chen, L., Zhang, K., He, J., Cai, X.G., Xu, W., Liu, J.H., 2016. Performance and mechanism of hierarchically porous Ce-Zr oxide nanospheres encapsulated calcium alginate beads for fluoride removal from water. RSC Adv. https://doi.org/10.1039/c6ra01337f
10. Chen, P., Zhang, W., Li, M., Ai, P., Tian, L., Jiang, H., 2016. Facile synthesis of magnetic La-Zr composite as high effective adsorbent for fluoride removal. RSC Adv. https://doi.org/10.1039/c5ra27929a
11. Deng, S., Liu, H., Zhou, W., Huang, J., Yu, G., 2011. Mn-Ce oxide as a high-capacity adsorbent for fluoride removal from water. J. Hazard. Mater. https://doi.org/10.1016/j.jhazmat.2010.12.024
12. Gao, C., Yu, X.Y., Luo, T., Jia, Y., Sun, B., Liu, J.H., Huang, X.J., 2014. Millimeter-sized Mg-Al-LDH nanoflake impregnated magnetic alginate beads (LDH-n-MABs): A novel bio-based sorbent for the removal of fluoride in water. J. Mater. Chem. A. https://doi.org/10.1039/c3ta13526h
13. Ghosh, A., Chakrabarti, S., Biswas, K., Ghosh, U.C., 2014. Agglomerated nanoparticles of hydrous Ce(IV) + Zr(IV) mixed oxide: Preparation, characterization and physicochemical aspects on fluoride adsorption. Appl. Surf. Sci. https://doi.org/10.1016/j.apsusc.2014.04.095
14. Hamayun, M., Mahmood, T., Naeem, A., Muska, M., Din, S.U., Waseem, M., 2014. Equilibrium and kinetics studies of arsenate adsorption by FePO4. Chemosphere. https://doi.org/10.1016/j.chemosphere.2013.10.075
15. Liu, H., Deng, S., Li, Z., Yu, G., Huang, J., 2010. Preparation of Al-Ce hybrid adsorbent and its application for defluoridation of drinking water. J. Hazard. Mater. https://doi.org/10.1016/j.jhazmat.2010.03.021
16. Mohammadian, S., Ghanemi, K., Nikpour, Y., 2016. Competitive adsorption of phthalate esters on marine surface sediments: kinetic, thermodynamic, and environmental considerations. Environ. Sci. Pollut. Res. https://doi.org/10.1007/s11356-016-7723-9
17. Mohan, S., Kumar, V., Singh, D.K., Hasan, S.H., 2016. Synthesis and characterization of rGO/ZrO 2 nanocomposite for enhanced removal of fluoride from water: kinetics, isotherm, and thermodynamic modeling and its adsorption mechanism. RSC Adv. https://doi.org/10.1039/C6RA15460C
18. Mukhopadhyay, K., Ghosh, A., Das, S.K., Show, B., Sasikumar, P., Chand Ghosh, U., 2017. Synthesis and characterisation of cerium(IV)-incorporated hydrous iron(III) oxide as an adsorbent for fluoride removal from water. RSC Adv. https://doi.org/10.1039/c7ra00265c
19. Podder, M.S., Majumder, C.B., 2016. Application of granular activated carbon/MnFe<inf>2</inf>O<inf>4</inf> composite immobilized on C. glutamicum MTCC 2745 to remove As(III) and As(V): Kinetic, mechanistic and thermodynamic studies. Spectrochim. Acta - Part A Mol. Biomol. Spectrosc. https://doi.org/10.1016/j.saa.2015.08.022
20. Ranjan, D., Talat, M., Hasan, S.H., 2009. Biosorption of arsenic from aqueous solution using agricultural residue "rice polish." J. Hazard. Mater. https://doi.org/10.1016/j.jhazmat.2008.12.013
21. Saha, I., Ghosh, A., Nandi, D., Gupta, K., Chatterjee, D., Ghosh, U.C., 2015. β-

Cyclodextrin modified hydrous zirconium oxide: Synthesis, characterization and defluoridation performance from aqueous solution. Chem. Eng. J. https://doi.org/10.1016/j.cej.2014.11.039
22. Saha, I., Kanrar, S., Gupta, K., Show, B., Nandi, D., Biswas, K., Manna, B., Chatterjee, D., Ghosh, U.C., 2016. Tuned synthesis and characterizational insight into β-cyclodextrin amended hydrous iron-zirconium hybrid oxide: A promising scavenger of fluoride in aqueous solution. RSC Adv. 6, 93842–93854. https://doi.org/10.1039/c6ra16567b
23. Sharma, Y.C., Weng, C.H., 2007. Removal of chromium(VI) from water and wastewater by using riverbed sand: Kinetic and equilibrium studies. J. Hazard. Mater. https://doi.org/10.1016/j.jhazmat.2006.08.078
24. Shortt, H.E., Pandit, C.G., Raghavachari, T.N.S., 1937. Endemic Fluorosis in the Nellore District of South India. Ind. Med. Gaz. 72, 396–398.
25. Singh, D.K., Kumar, V., Mohan, S., Hasan, S.H., 2017. Polylysine Functionalized Graphene Aerogel for the Enhanced Removal of Cr(VI) through Adsorption: Kinetic, Isotherm, and Thermodynamic Modeling of the Process. J. Chem. Eng. Data. https://doi.org/10.1021/acs.jced.7b00188
26. Singh, D.K., Kumar, V., Singh, V.K., Hasan, S.H., 2016a. Modeling of adsorption behavior of the amine-rich GOPEI aerogel for the removal of As(III) and As(v) from aqueous media. RSC Adv. https://doi.org/10.1039/c6ra10518a
27. Singh, D.K., Mohan, S., Kumar, V., Hasan, S.H., 2016b. Kinetic, isotherm and thermodynamic studies of adsorption behaviour of CNT/CuO nanocomposite for the removal of As(iii) and As(v) from water. RSC Adv. https://doi.org/10.1039/c5ra20601d
28. Tang, D., Zhang, G., 2016. Efficient removal of fluoride by hierarchical Ceâ€“Fe bimetal oxides adsorbent: Thermodynamics, kinetics and mechanism. https://doi.org/10.1016/j.cej.2015.08.019
29. Tomar, V., Prasad, S., Kumar, D., 2013. Adsorptive removal of fluoride from water samples using Zr-Mn composite material. Microchem. J. https://doi.org/10.1016/j.microc.2013.04.007
30. Wen, S., Wang, Y., Dong, S., 2015. Performance and characteristics of fluoride adsorption using nanomagnetite graphite-La adsorbent. RSC Adv. https://doi.org/10.1039/c5ra15215a
31. Wu, X., Zhang, Y., Dou, X., Yang, M., 2007. Fluoride removal performance of a novel Fe-Al-Ce trimetal oxide adsorbent. Chemosphere. https://doi.org/10.1016/j.chemosphere.2007.05.075
32. Zhao, B., Zhang, Y., Dou, X., Wu, X., Yang, M., 2012. Granulation of Fe-Al-Ce trimetal hydroxide as a fluoride adsorbent using the extrusion method. Chem. Eng. J. https://doi.org/10.1016/j.cej.2012.01.085
33. Zhu, J., Lin, X., Wu, P., Zhou, Q., Luo, X., 2015. Fluoride removal from aqueous solution by Al(III)-Zr(IV) binary oxide adsorbent. Appl. Surf. Sci. https://doi.org/10.1016/j.apsusc.2015.09.012

Future Work

Following sections are yet to be completed:

- Column Study- Modelling of column data to evaluate the column adsorption performance.
- Column data validation with the help of ANN(Artificial Neural Networking Model)
- Installation of "proto-type" Filter units in selective areas of Bankura-II block under Bankura District, WB, to provide safe drinking in domestic range.

Topic	Present status	Outcome
Literature review		
Geochemical aspect of occurrence of fluoride in Groundwater	ongoing	---
Fluoride removal techniques	ongoing	---
Adsorbents and their application on fluoride removal purpose	ongoing	---
Research Work		
Preparation of [Fe(III)–Ce (IV)] named as CIHFO and application for fluoride removal	Characterisation of this material completed	Data is used in research paper and published.
	Batch adsorption study to evaluate fluoride removal efficacy completed	
Surface modification of CIHFO with graphene oxide and application	**Done**	Data is used in research paper, Manuscript submitted.
Surface modification of CIHFO with β–Cyclodextrin and application	**Done**	Data analysis and preparation of original research paper under progress
CIHFO packed Column operation for fluoride removal	Experimental portion completed	Data analysis and preparation of original research paper under progress
	Modelling and data analysis under process	
Filter unit development	Design and fabrication done	Outcome will be incorporated in thesis
	Field installation not yet done	
Writing of Thesis		
Compilation of data & results	Oct 2018- Dec 2018	
Finish writing thesis	February 2018	
Correction & submission	March 2018	

Table 1: Estimated kinetic parameters for fluoride adsorption reactions with CIHFO, GO-CIHFO and βC-CIHFO at different concentration of Fluoride with solution pH 7.0 and at temperature 303K.

Kinetics Equation	Parameters	βC-CIHFO			GO-CIHFO			CIHFO		
		Fluoride concentration (mg. L^{-1})			Fluoride concentration (mg. L^{-1})			Fluoride concentration (mg. L^{-1})		
		5	10	15	5	10	15	10	15	20
Pseudo-First order	k_1 (min^{-1})	0.028	0.028	0.015	0.108	0.077	0.058	0.06	0.10	0.14
	Q_t (mg g^{-1})	18.43	25.78	20.12	10.38	13.45	16.51	12.34	14.70	16.3
	R^2	0.89	0.92	0.89	0.92	0.98	0.93	0.99	0.99	0.96
	χ^2	4.55	5.971	4.30	0.484	0.270	2.270	0.08	0.27	1.24
Pseudo-second order	k_2 (g mg^{-1} min^{-1})	0.001	0.001	0.007	0.013	0.006	0.002	0.005	0.007	0.010
	Q_t(mg g^{-1})	22.15	30.69	25.19	11.29	14.91	18.30	14.40	16.37	17.98
	R^2	0.98	0.95	0.95	0.977	0.99	0.95	0.99	0.99	0.97
	χ^2	0.85	3.83	2.40	0.151	0.161	1.45	0.17	0.31	0.82
Intra-particle diffusion Model	K_{id}($gmg^{-1}min^{0.5}$)	1.723	3.316	2.022	1.105	1.43	1.14	1.77	2.54	2.82
	C	1.073	2.153	-3.711	2.086	2.38	4.63	0.258	0.113	1.27
	R^2	0.95	0.96	0.98	0.84	0.89	0.92	0.96	0.94	0.88
Elovich Model	a(mg/g min)	4.6756	2.421	6.293	1.803	3.27	3.25	2.421	2.370	2.365
	b (g/mg)	-3.482	1.941	-12.67	2.302	-0.089	1.09	1.941	2.803	6.666
	R^2	0.99	0.92	0.95	0.972	0.98	0.98	0.92	0.96	0.97
Richenberg Model	$\beta_t \times 10^{-2}$ (cm^2 s^{-1})	0.595	0.583	0.41	0.97	1.55	1.13	2.137	1.261	2.462
	R^2	0.96	0.98	0.98	0.95	0.94	0.95	0.94	0.90	0.83
	$D_i \times 10^{-6}$(cm^2 s^{-1})	1.59	1.56	1.098	2.59	4.15	3.02	5.72	3.37	0.659
	D_1 (cm^2 s^{-1})	0.067	0.064	0.059	0.0548	0.0631	0.0644	0.0602	0.04125	0.041
	D_2 (cm^2 s^{-1})	-0.183	-0.179	-0.121	-0.040	-0.052	-0.030	-0.189	-0.131	-0.264

Table 2: Estimated kinetic parameters for fluoride adsorption reactions with CIHFO (Fluoride concentration -10 $mg.L^{-1}$), GO-CIHFO and βC-CIHFO at different at different temperature (Fluoride concentration -15$mg.L^{-1}$) with solution pH 7.0.

Kinetics Equation	Parameters	βC-CIHFO			GO-CIHFO			CIHFO		
		Temperature (K)			Temperature (K)			Temperature (K)		
		288	303	313	288	303	313	293	303	313
Pseudo-First order	k_1 (min^{-1})	0.153	0.015	0.103	0.0311	0.058	0.044	0.05	0.06	0.07
	Q_t ($mg\ g^{-1}$)	29.95	20.12	24.50	18.35	16.51	12.53	16.28	12.56	11.63
	R^2	0.93	0.89	0.91	0.95	0.93	0.96	0.99	0.99	0.986
	χ^2	6.48	4.30	6.45	2.06	2.27	0.93	0.23	0.11	0.30
Pseudo-second order	k_2 ($g\ mg^{-1}\ min^{-1}$)	0.006	0.007	0.005	0.001	0.002	0.003	0.003	0.005	0.006
	Q_t($mg\ g^{-1}$)	32.14	25.19	26.46	21.71	18.30	14.51	19.20	14.61	13.48
	R^2	0.97	0.95	0.97	0.97	0.95	0.93	0.99	0.99	0.97
	χ^2	2.14	2.40	2.22	1.07	1.45	1.793	0.32	0.17	0.47
Intra-particle diffusion Model	K_{id}($gmg^{-1}\ min^{0.5}$)	2.427	2.022	1.565	1.50	1.14	1.126	2.441	1.77	2.782
	C	9.765	-3.711	10.07	2.27	4.63	0.516	-0.595	0.258	0.934
	R^2	0.94	0.98	0.96	0.98	0.92	0.89	0.95	0.96	0.90
Elovich Model	a(mg/g min)	4.911	6.293	5.160	4.08	3.25	3.65	4.112	2.421	1.89
	b (g/mg)	9.479	-12.67	3.654	-2.09	1.09	-3.50	-1.728	1.941	3.326
	R^2	0.95	0.95	0.95	0.96	0.98	0.97	0.97	0.92	0.95
Mass Transfer	$\beta_1 \times 10^{-2}$ ($cm^2\ s^{-1}$)	0.247	0.667	1.17	0.267	0.667	0.829	2.43	4.18	0.35

	R^2	**0.92**	**0.93**	**0.98**	**0.87**	**0.90**	**0.91**	**0.94**	**0.99**	**0.90**
Richenberg Model	**$\beta_t \times 10^{-2}$ ($cm^2\ s^{-1}$)**	**2.26**	**0.41**	**1.257**	**0.724**	**1.13**	**1.46**	**1.352**	**2.137**	**0.534**
	R^2	**0.93**	**0.98**	**0.97**	**0.98**	**0.95**	**0.99**	**0.93**	**0.94**	**0.94**
	$D_i \times 10^{-6}$($cm^2\ s^{-1}$)	**0..60**	**1.098**	**3.36**	**0.193**	**3.02**	**3.91**	**3.62**	**5.72**	**1.43**
	D_1 ($cm^2\ s^{-1}$)	**0.053**	**0.059**	**0.048**	**0.077**	**0.064**	**0.163**	**0.078**	**0.0602**	**0.076**
	D_2 ($cm^2\ s^{-1}$)	**-0.48**	**-0.121**	**-0.354**	**0.0248**	**0.0308**	**0.109**	**-0.215**	**-0.189**	**-0.226**

Table 3: Isotherm parameters of fluoride adsorption reactions with CIHFO, GO- CIHFO and βC-CIHFO at pH 7.0(±0.2) at different temperatures

Isotherm Model	Parameters	βC-CIHFO				GO-CIHFO				CIHFO		
		Temperature (K)				Temperature (K)				Temperature (K)		
		288	303	313	323	288	303	313	323	293	303	313
Langmuir	Q_m (mg g^{-1})	51.3	52.32	73.949	107.62	56.02	80.42	97.02	136.24	32.62	22.55	16.91
	K_L (L mg^{-1})	0.05	0.071	0.0492	0.030	0.093	0.027	0.022	0.015	0.13	0.66	2.18
	R^2	0.91	0.93	0.97	0.98	0.95	0.97	0.98	0.97	0.96	0.88	0.84
Freundlich	n	2.18	2.417	2.0273	1.6750	2.55	1.69	1.58	1.40	3.10	4.47	7.57
	1/n	0.45	0.41	0.49	0.59	0.39	0.59	0.63	0.71	0.322	0.22	0.132
	K_F (mg g^{-1})	6.34	8.307	7.853	6.439	10.38	4.71	4.75	3.81	8.58	10.88	11.25
	R^2	0.97	0.98	0.98	0.98	0.95	0.98	0.97	0.99	0.99	0.99	0.98
Dubinin–Radushkevich	Q_m (mol kg^{-1})	5.09	6.808	8.536	18.35	7.158	9.02	16.60	19.01	3.05	2.07	1.29
	β (mol^2 kJ^{-1}) × 10^{-3}	-4.89	-5.05	-4.83	-6.49	-5.13	-5.99	-7.22	-7.06	3.14	2.08	1.21
	E_{DR} (kJ mol^{-1})	10.11	9.95	10.17	8.77	9.87	9.13	8.32	8.41	12.61	15.50	20.32
	R^2	0.94	0.98	0.98	0.99	0.97	0.93	0.99	0.97	0.60	0.96	0.98

Table 4: Thermodynamic parameters for fluoride adsorption reaction with of all three adsorbents and pH = 7.0 (±0.2)

Material Name	**Fluoride concentration (mg L^{-1})**	**ΔG° (kJ mol^{-1}) at different Temperatures (K)**				**ΔH° (kJmol^{-1})**	**ΔS° (J$mol^{-1}K^{-1}$)**
		288	**303**	**313**	**323**		
βC-CIHFO	35	-9.100	-9.880	-10.940	-18.08	13.34	77.47
	60	-8.555	-9.268	-10.169	-11.104	12.26	71.80
GO-CIHFO	35	-9.68	-10.02	-10.72	-11.43	11.22	70.16
	60	-9.22	-9.61	-10.27	-10.97	13.76	76.74
Material Name	**Fluoride concentration (mg L^{-1})**	**ΔG° (kJ mol^{-1}) at different Temperatures (K)**				**ΔH° (kJmol^{-1})**	**ΔS° (J$mol^{-1}K^{-1}$)**
		293	**303**	**313**	**323**		
CIHFO	25	-11.941	-11.698	-10.971	--------	-25.924	-47.411
	35	-10.913	-10.011	-9.160	---------	-36.279	-86.537

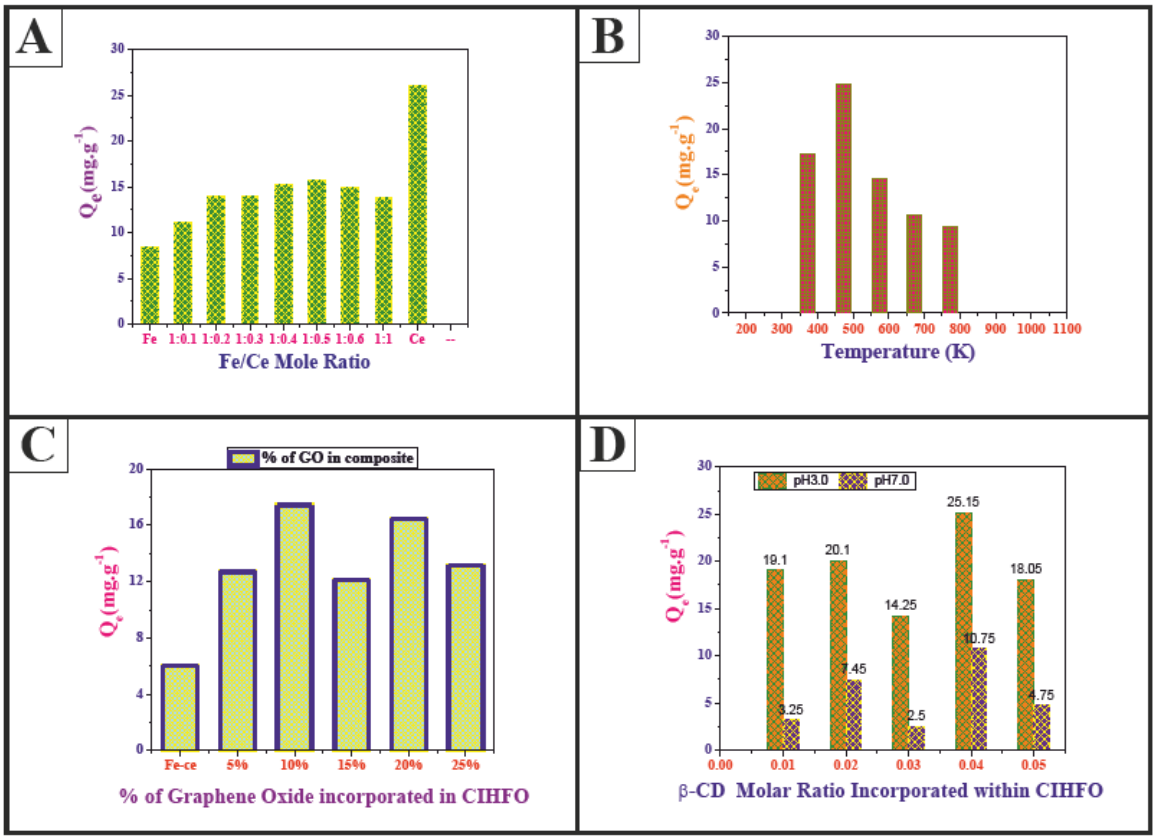

Fig.1: (A) Effect on the variation of Fe/Ce mole ratio and **(B)** calcined temperature upon fluoride adsorption capacity of Fe/Ce (1.0:0.5) nanocomposite (CIHFO) **(C)** Study of Percentage variation of Graphene Oxide in association within CIHFO and its effect upon fluoride adsorption capacity; **(D)** Study of β CD Molar ratio Incorporation within CIHFO and its effect upon fluoride adsorption capacity.

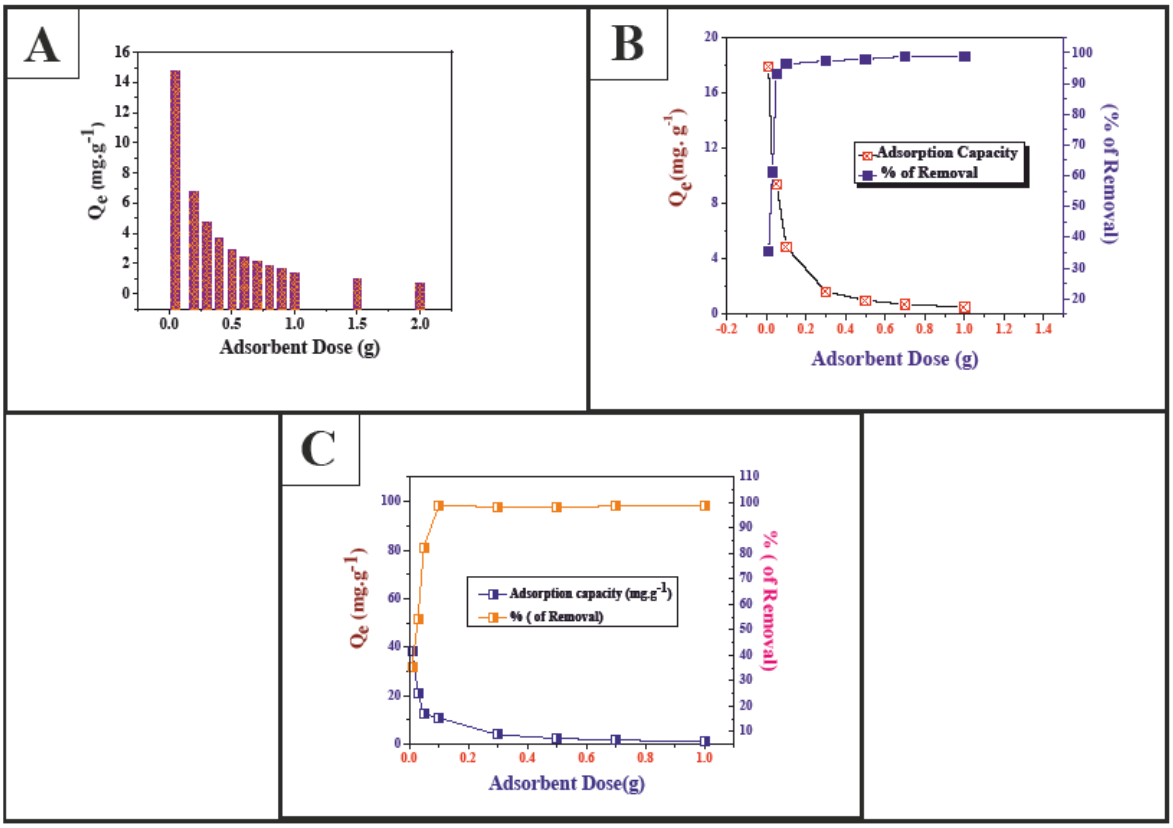

Fig. 2: Effect of adsorbent dose of three synthesized adsorbents **(A)** CIHFO; **(B)** GO-CIHFO and **(C)** βC-CIHFO on fluoride removal at pH 7.0 (±2) and temperature 303 K (±2°C) with contact time 120 min.

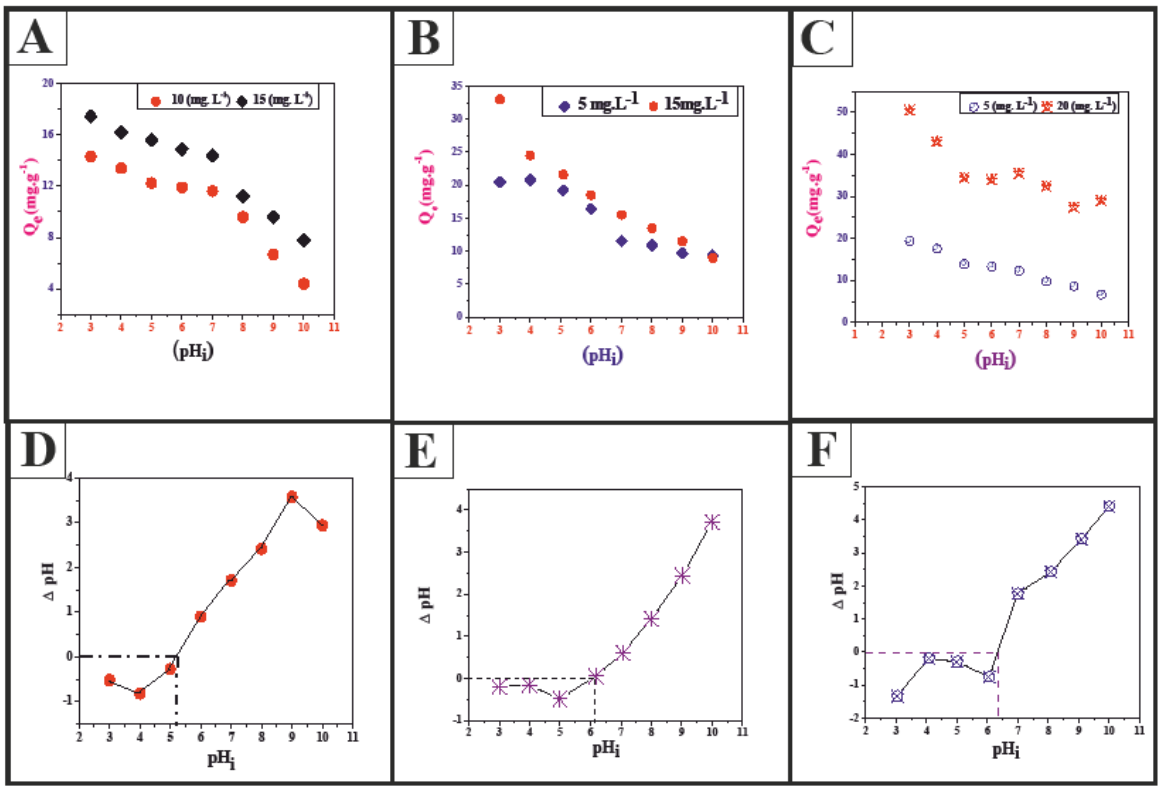

Fig. 3: (A)-(C) shows the effect of initial solution pH on the adsorption of fluoride over the surfaces of adsorbent at 303 K from two different fluoride solution concentration for three different adsorbents CIHFO, GO-CIHFO and βC-CIHFO respectively; **(D)–(F)** represent the Plots of Δ pH versus pH_i for the estimation of pH_{ZPC} of three different adsorbents CIHFO, GO-CIHFO and βC-CIHFO respectively.

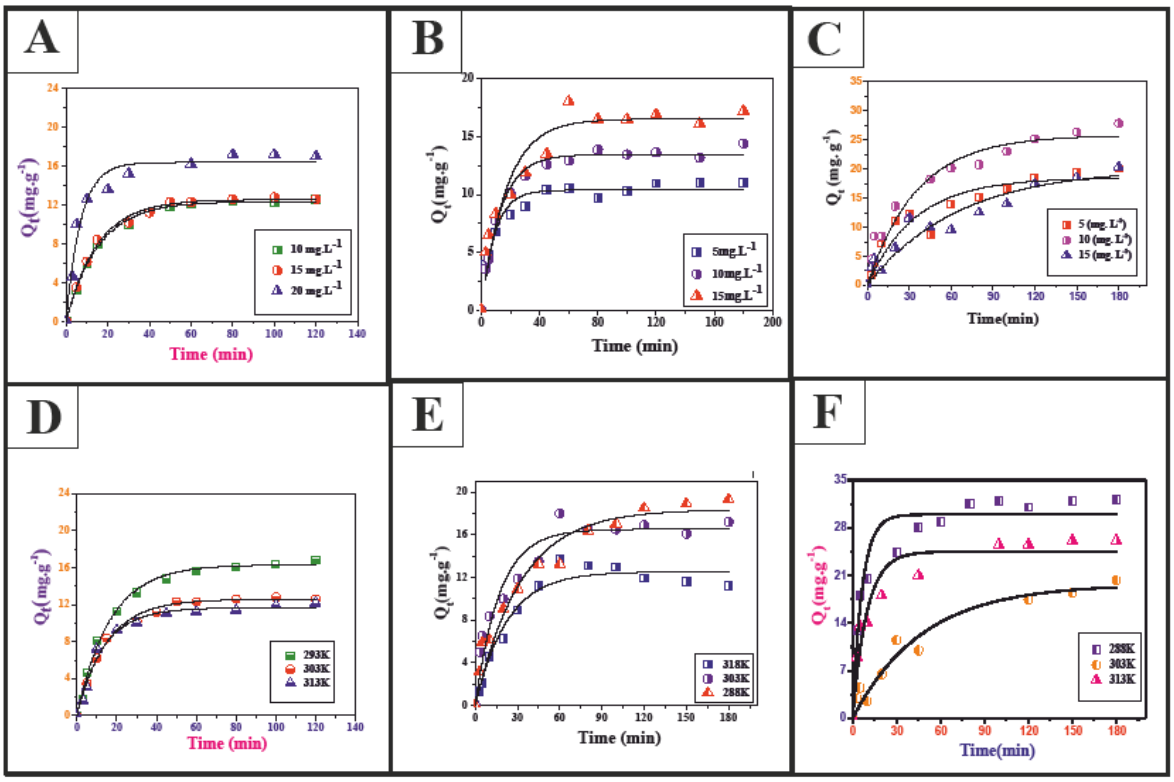

Fig. 4: (A)–(C) The plots of fluoride adsorption capacity at any time, Q_t (mg.g^{-1}) versus time, t(min) including non-linear pseudo first order (—) at three concentration at temperature 303K ionic strength = 1M) and pH 7.0 for three different adsorbents CIHFO, GO-CIHFO and βC-CIHFO respectively;**(D) - (F)** The plots of fluoride adsorption capacity at any time, Q_t (mg. g^{-1}) versus time, t (min) including non-linear pseudo first order (—) at three temperatures with active fluoride concentration 15 mg.L^{-1} (ionic strength = 1M) at pH 7.0 for three different adsorbents CIHFO, GO-CIHFO and βC-CIHFO respectively.

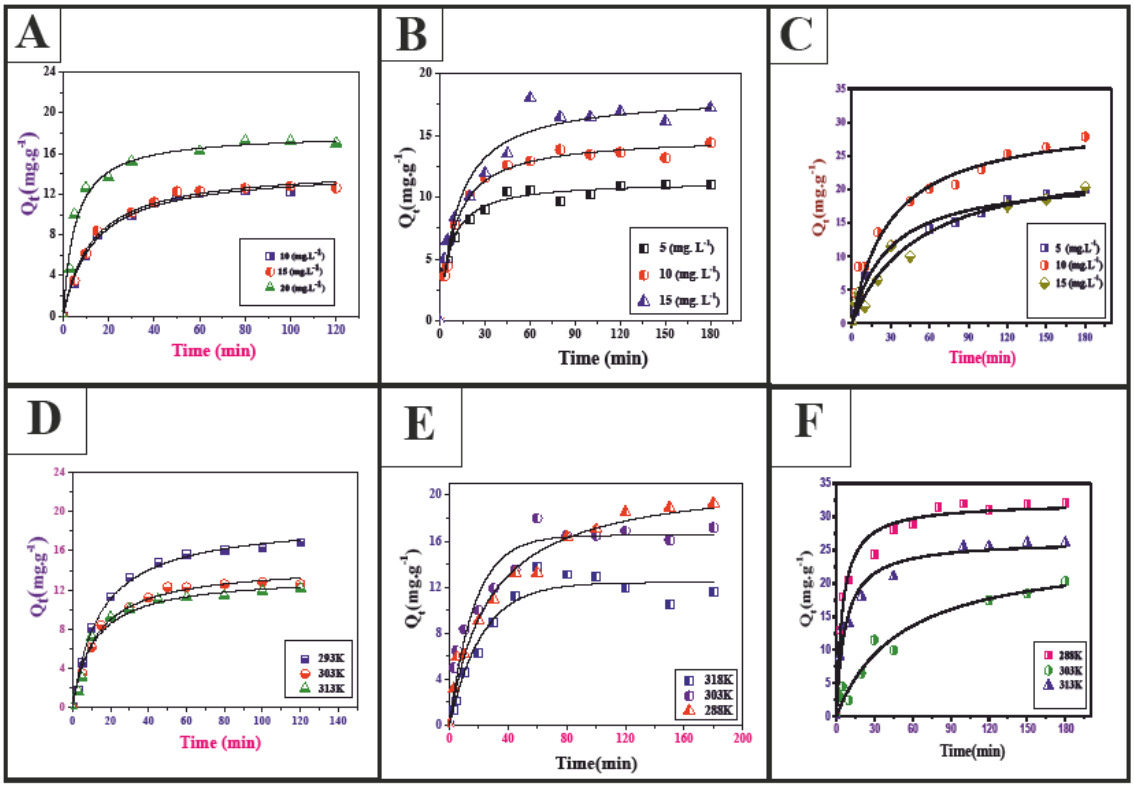

Fig. 5: (A) –(C) The plots of fluoride adsorption capacity at any time, Q_t (mg. g^{-1}) versus time, t (min) including non-linear pseudo second order (—) at three concentration at temperature 303K ionic strength = 1M) and pH 7.0 for three different adsorbents CIHFO, GO-CIHFO and βC-CIHFO respectively;**(D) - (F)** The plots of fluoride adsorption capacity at any time, Q_t (mg. g^{-1}) versus time, t (min) including non-linear pseudo second order (—) at three temperatures with active fluoride concentration 15 mg. L^{-1} (ionic strength = 1M) at pH 7.0 for three different adsorbents CIHFO, GO-CIHFO and βC-CIHFO respectively.

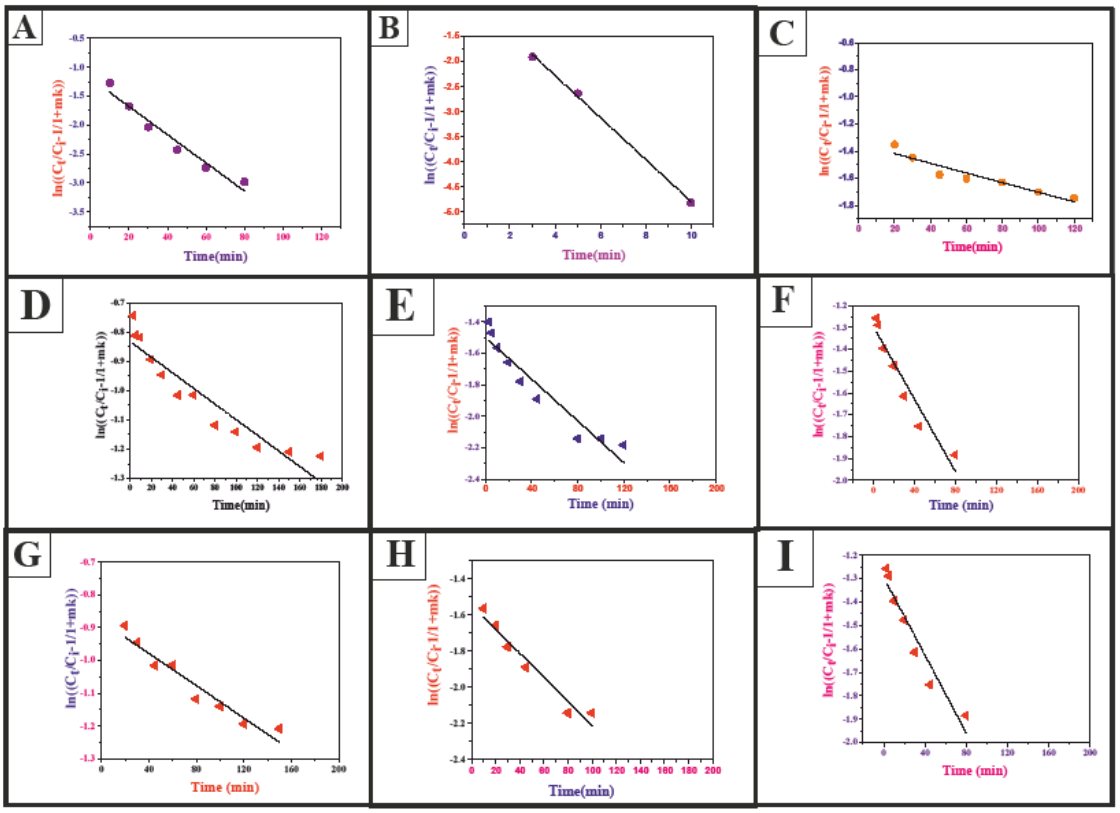

Fig.6: (A)-(I) depicting mass transfer at three different temperature (288 K/293K, 303 K and 313 K) with active fluoride concentration 15 mg.L^{-1} (ionic strength = 1M) and at pH 7.0 for three different adsorbents CIHFO, GO-CIHFO and βC-CIHFO respectively.

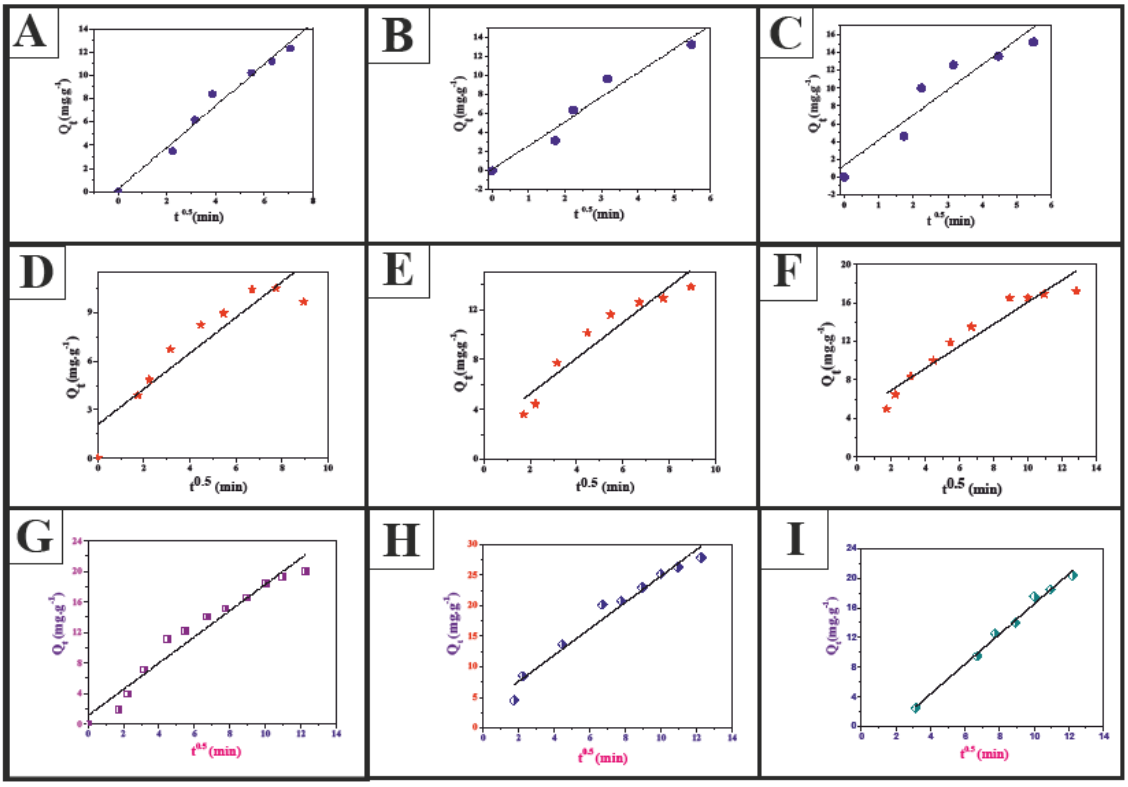

Fig.7: (A)-(I) The plots of fluoride adsorption capacity at any time, Q_t (mg. g^{-1}) versus time, t (min) depicting intra particle diffusion model at three different concentrations (at temperature 303K (ionic strength = 1M) and at pH 7.0 for three different adsorbents CIHFO, GO-CIHFO and βC-CIHFO respectively.

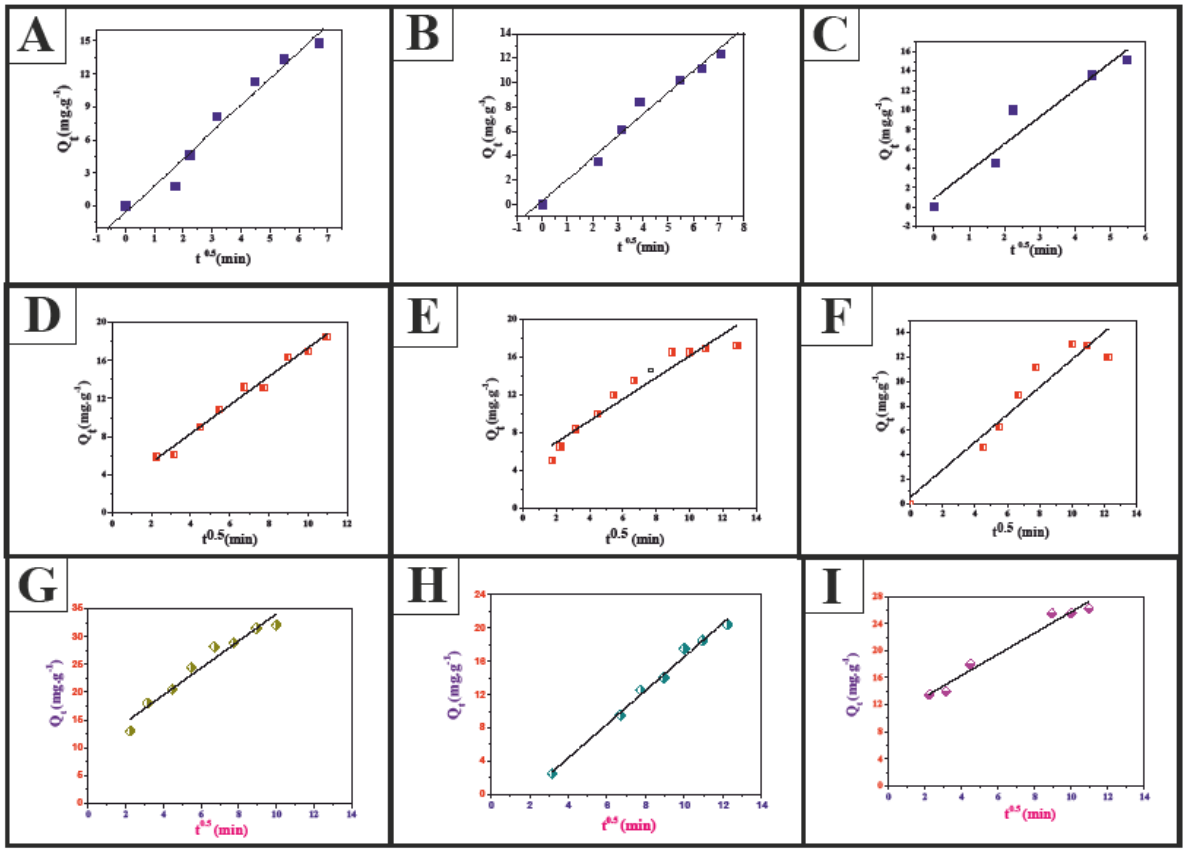

Fig.8: (A)-(I) The plots of fluoride adsorption capacity at any time, Q_t ($mg.g^{-1}$) versus time, t (min) depicting intra particle diffusion model at three different temperature with active fluoride concentration 15 $mg.L^{-1}$ (ionic strength = 1M) and at pH 7.0 for three different adsorbents CIHFO, GO-CIHFO and βC-CIHFO respectively.

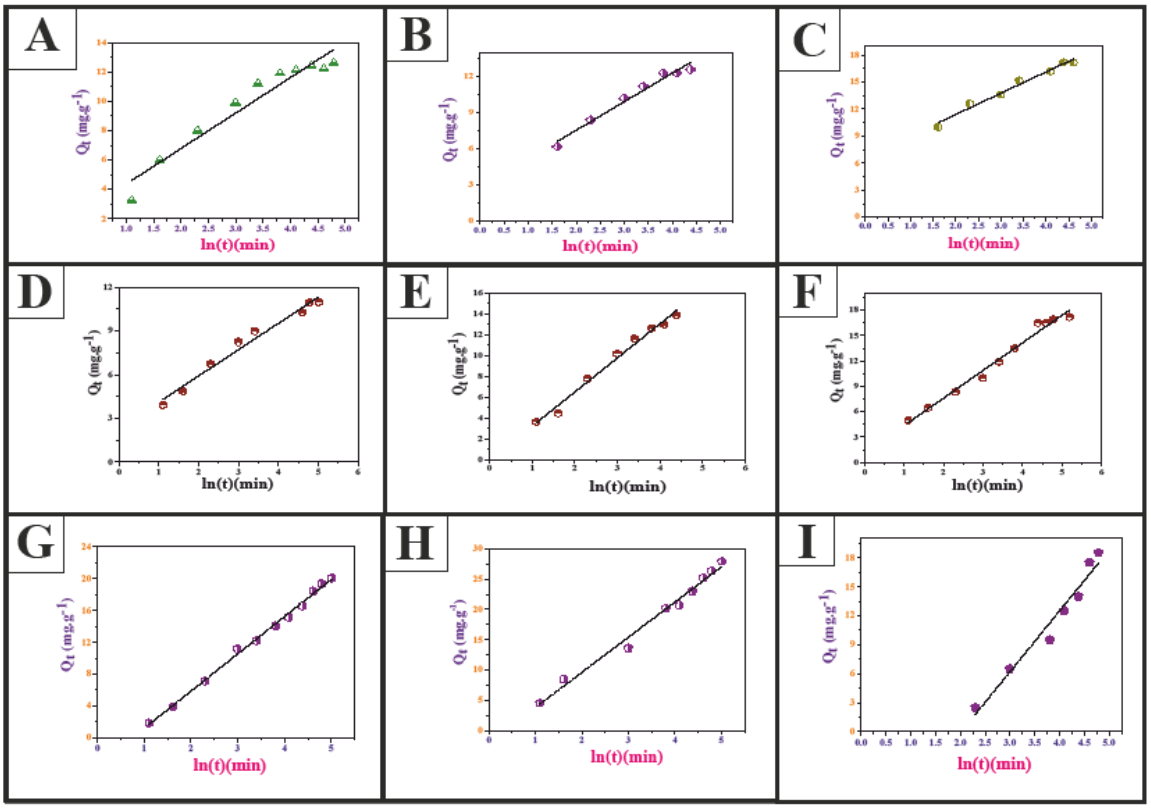

Fig. 9: (A)-(I) The plots Q_t (mg. g^{-1}) versus ln(t)(min) depicting Elovich Model at three different concentrations at temperature 303K (ionic strength = 1M) and at pH 7.0 for three different adsorbents CIHFO, GO-CIHFO and βC-CIHFO respectively.

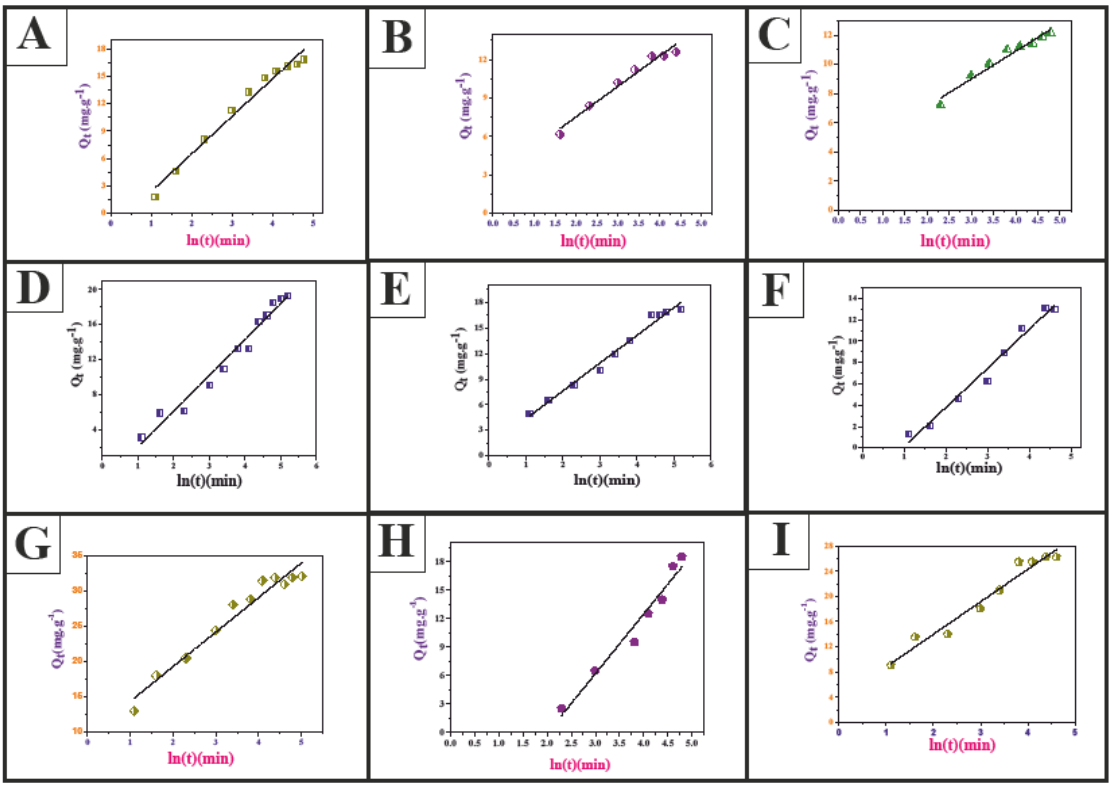

Fig.10: (A)-(I) The plots Q_t (mg. g^{-1}) versus ln(t)(min) depicting Elovich Model at three different temperature with active fluoride concentration 15 $mg.L^{-1}$ (ionic strength = 1M) and at pH 7.0 for three different adsorbents CIHFO, GO-CIHFO and βC-CIHFO respectively.

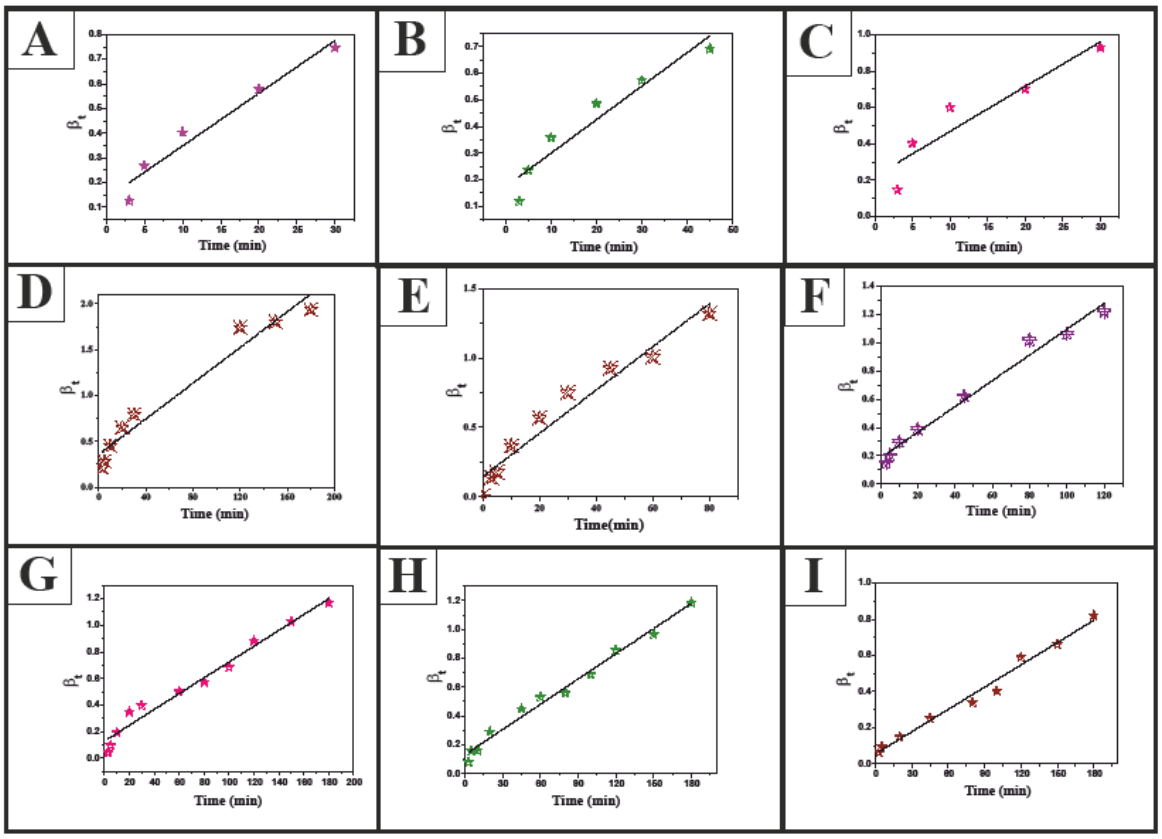

Fig.11: (A)-(I) The plots β_t versus time, t (min) depicting Richenberg Model at three different concentrations at temperature 303K (ionic strength = 1M) and at pH 7.0 for three different adsorbents CIHFO, GO-CIHFO and βC-CIHFO respectively.

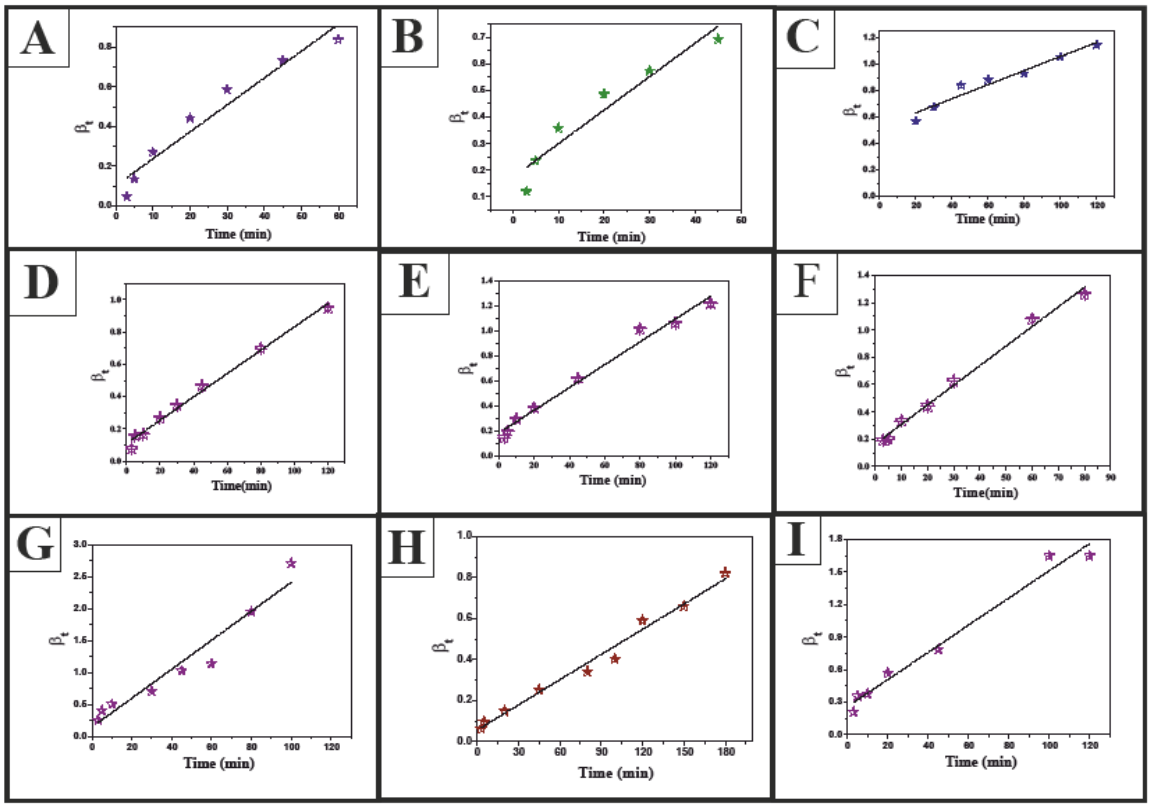

Fig.12: (A)-(I) The plots β_t versus time, t(min) depicting Richenberg Model at three different temperature with active fluoride concentration 15 mg.L^{-1} (ionic strength = 1M) and at pH 7.0 for three different adsorbents CIHFO, GO-CIHFO and βC-CIHFO respectively.

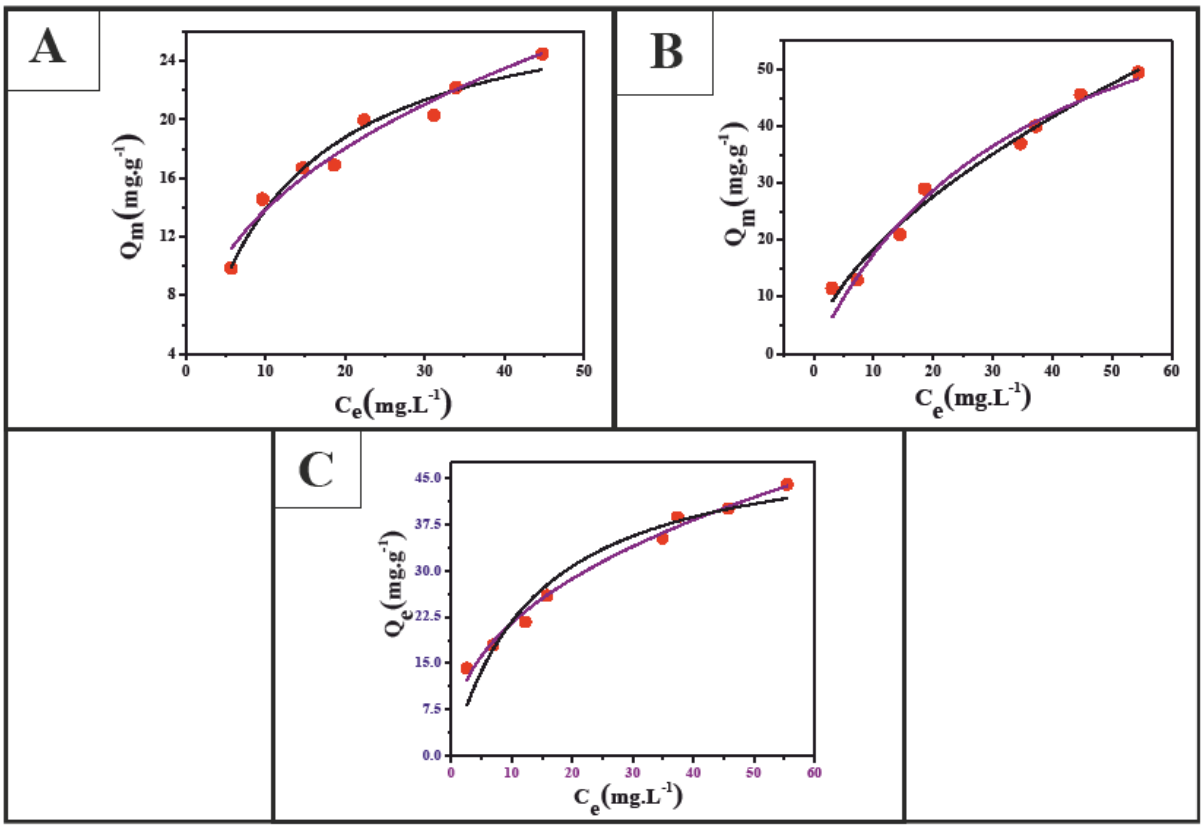

Fig.13: (A)–(C) Plots of equilibrium adsorption capacity (Q_e) versus equilibrium concentration (C_e) of fluoride and nonlinear fitting of data with Langmuir and Freundlich models for adsorption of fluoride on adsorbent at pH 7.0 at temperature 303K for three different adsorbents CIHFO, GO-CIHFO and βC-CIHFO respectively.

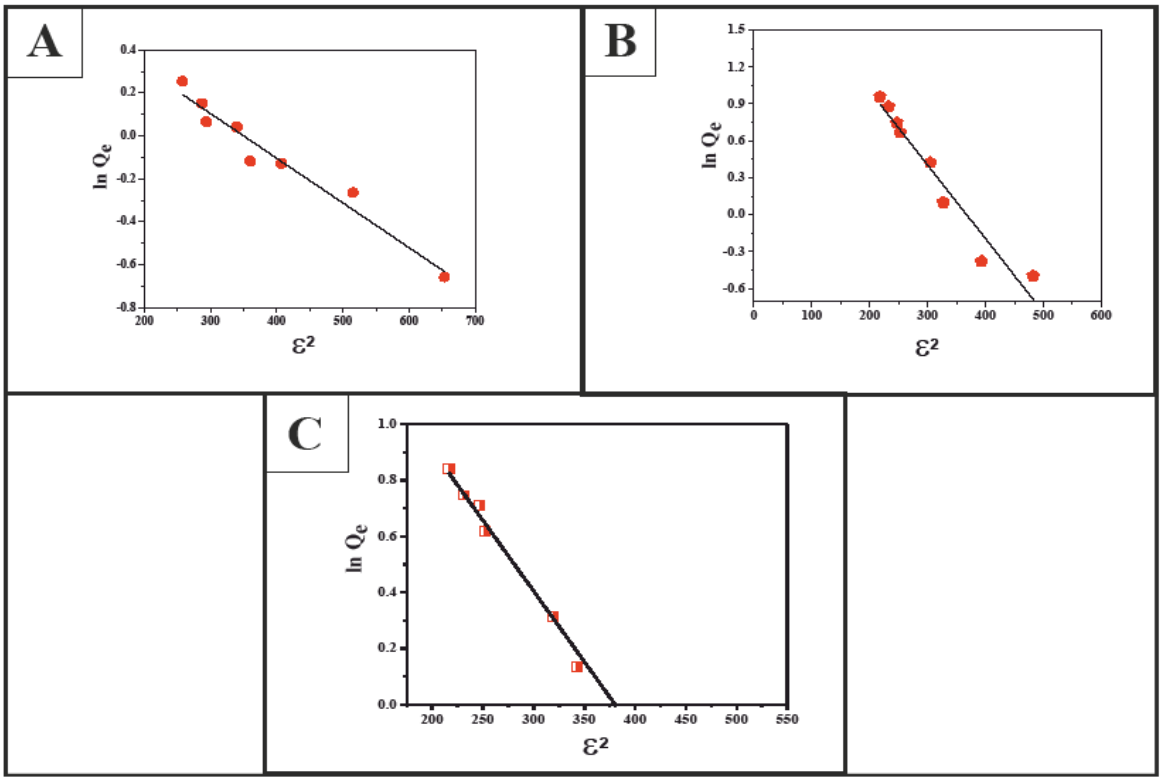

Fig.14: (A)-(C) represent the plots of ln Q_e versus ε^2 for D-R isotherm of three adsorbents CIHFO, GO-CIHFO and βC-CIHFO respectively at temperature 303K and pH 7.0.

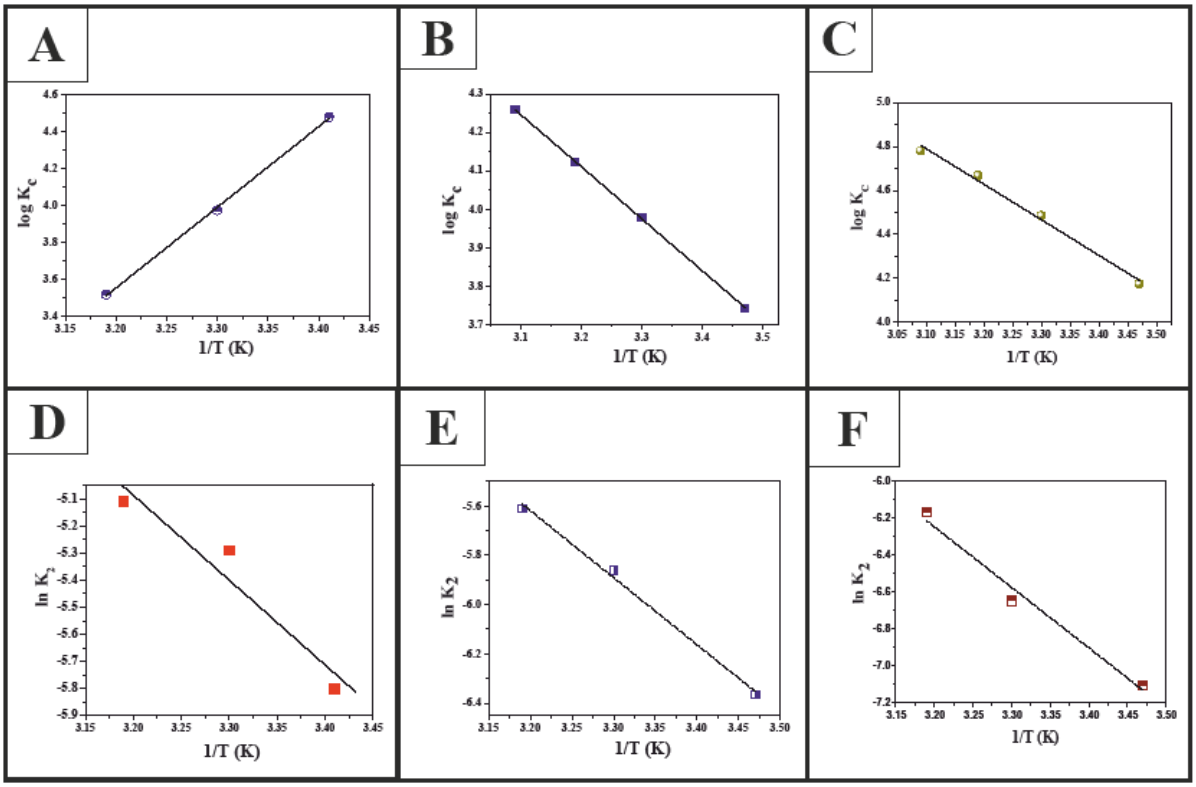

Fig.15: (A)-(C) represent Van't Hoff plots for the adsorption of fluoride with CIHFO;GO-CIHFO and βC-CIHFO respectively with solution pH 7.0; **(D)-(F)** rendering the plots of ln k_2 versus 1/T (K) for the activation energy of fluoride adsorption reaction with CIHFO, GO-CIHFO and βC-CIHFO at solution pH 7.0 respectively.

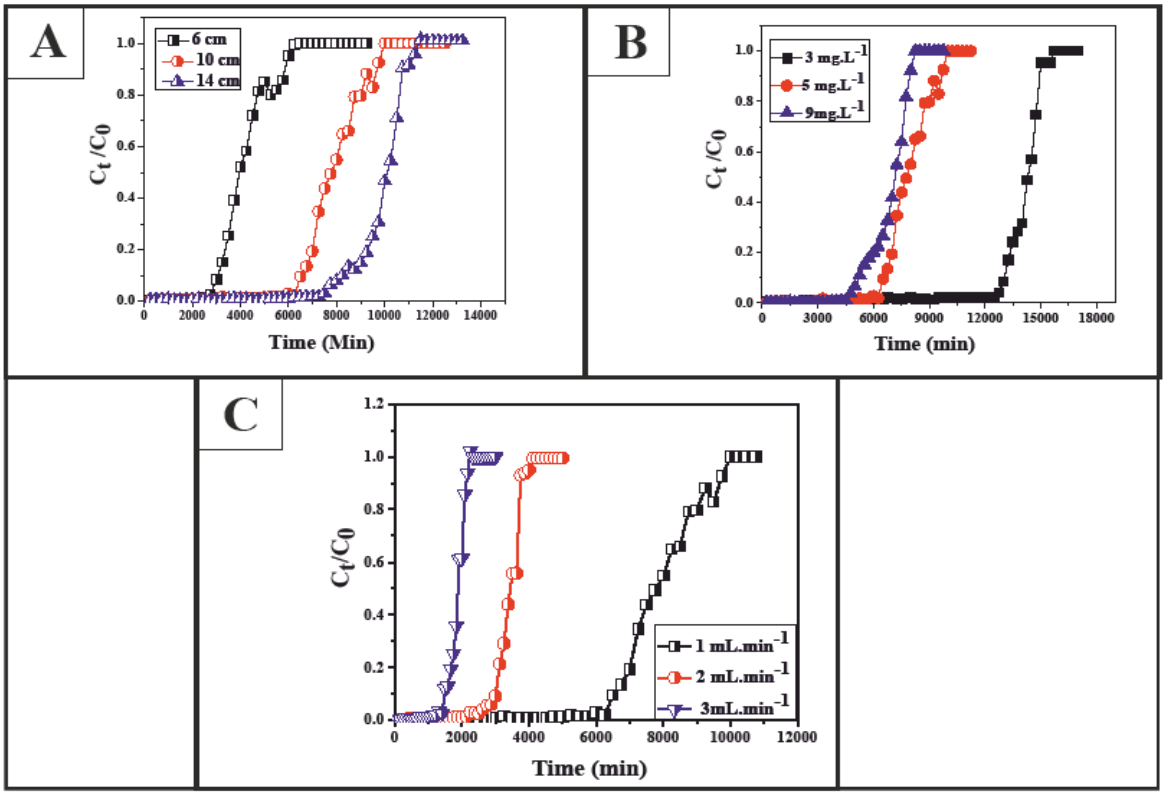

Fig.16: The plots of C_t/C_0 versus time required for treatment of fluoride enriched groundwater by CIHFO packed fixed-bed depth in lab-bench scale; **(A)** at different Bed-Heights; **(B)** at different conc. of fluoride and **(C)** at different effluent discharge rate.

Annexure –I

1. Batch Adsorption Study

A systematic batch adsorption study is essential step to establish an adsorbent as a good water purifier. To achieve this goal, a measured volume fluoride solution (50 mL/100mL) with desired initial fluoride concentration (C_i, $mg.L^{-1}$) was taken in 250 ml polyethylene (PE) bottle along with a certain mass (0.01g/0.05g) of adsorbent (except dose variation study) and agitated at 250 (± 5) rpm using a thermostatic shaker for two hours (except time dependent experiment).The filtrate obtained by immediate filtration process was analysed to evaluate residual concentration of fluoride (C_f, $mg.L^{-1}$).

pH of any solution is considered as a crucial parameter that has immense impact upon any adsorption process. In present batch study, effect of the solution pH upon fluoride adsorption was explored independently in the pre-programmed pH_i 3.0 to 10.0 by a unit increment, with two different fluoride solutions (C_i: 5.0 and 15.0 $mg.L^{-1}$). The pH value of each test solutions was adjusted with 0.1 M HCl and 0.1 M NaOH solution, as per requirement, respectively.

Reaction kinetics for fluoride adsorption trials with adsorbent, were conducted with three separate concentrations of fluoride solution. Same experiment was also carried out in three different temperatures (288K, 303K and 313K) with a fixed fluoride concentration (15.0 mg. L^{-1}).

For equilibrium experiments, fluoride solution (C_i) ranged between 5.0 – 60.0 $mg.L^{-1}$ was taken for scheduled experiments at four temperatures, 288K, 303K, 313K,323K respectively, agitation time (2 hours) and speed 250(±5)rpm. The fluoride concentration at equilibrium (C_e, mg. L^{-1}) was analysed by ion-selective electrode and equilibrium capacity (Q_e, $mg.g^{-1}$) was calculated. Thermodynamic parameters (ΔS°, ΔH°, ΔG°) were evaluated from the results of equilibrium analysis.

Groundwater may also contain some ions like HPO_4^{2-}, SO_4^{2-}, HCO_3^-, NO_3^- and Cl^-. Adsorption of fluoride over adsorbent may be influenced by the presence of such ions. To evaluate the effects of these ions upon fluoride adsorption, batch experiments were conducted at neutral pH using the fluoride solution of C_i =10.0 mg. L^{-1} in the presence of different concentration levels of competing ions.

1.1. Adsorption capacity

Immediately after each experiment, the adsorbent particles were filtered through 0.45 µm membrane filter. The residual fluoride level left in each filtrate was analysed. The adsorbed amount of fluoride by adsorbent was calculated by application of the following mass balance equation (Eq. 1)(Mukhopadhyay et al., 2017)

$$Q_e = \left(C_i - C_f\right) \times \frac{V}{M} \qquad \text{(Eq. 1)}$$

Where Q_e is the adsorption capacity ($mg.g^{-1}$), V the volume of solution (L), M is the mass of adsorbent (g) used to carry out the batch experiments. And the significance of C_i and C_f have been given previously.

The removal percentage of fluoride by adsorbate was calculated (Podder and Majumder, 2016) as follows:

$$Re(\%) = \frac{(C_i - C_f)}{C_i} X\ 100 \qquad \text{(Eq. 2)}$$

1.2. Desorption and Reuse

For desorption study, in general, fluoride adsorption was first done with higher range of initial fluoride concentration. Fluoride containing adsorbent was then kept for air drying followed by subjected to desorption study by maintaining pH values (8-13) by addition of 0.1 M HCl and 0.1 M NaOH solution, as required, respectively. After achieving optimum pH level for defluoridation, the defluoridated adsorbent was carefully collected and this mostly fluoride free adsorbent then air dried and used for repeating the aforesaid adsorption-desorption study. The adsorbents were reused for as many as cycles as possible. Mass balance equation used for desorption and regeneration process are mentioned here in (Eq. 3) and in (Eq. 4)(Zhao et al., 2012).

Desorption Study

$$\frac{\text{The amount of Fluoride Desorbed}}{\text{The amount of Fluoride Adsorbed(same cycle)}} \text{ X } 100 \qquad \text{(Eq. 3)}$$

Regeneration and Recycling

$$\frac{\text{The amount of Fluoride adsorbed (Reuse)}}{\text{the amount of Fluoride adsorbed (the first cycle)}} \text{ X } 100 \qquad \text{(Eq. 4)}$$

1.3. Field validation

The purpose of this study is to development of an adsorbent that can be use as water purifier. In this context, field validation with optimised material is an essential step. To achieve this goal, water samples have been collected from different hand pump attached tube wells of Kashipur block, most adversely fluoride effected region of Purulia district, under the state of West Bengal, India. Fluoride concentration of collected water samples were analysed in laboratory by ion selective electrode and water sample with maximum fluoride concentration (Kharai village) was used for field validation (Mukhopadhyay et al., 2017).

2. Column Adsorption Experimental Set-up

Agglomerated nanoparticles (size: 140-290 μm) of CIHFO was packed uniformly into the glass column (height: ~ 59 cm, internal diameter, id: 2.30 cm, cross sectional area: 4.153 cm^2) over glass wool followed by glass beads and cotton to avoid void spaces, channels and cracks in fixed-beds and set up to the desired bed heights. Before conducting experiment, each fixed- bed was washed five times with de-ionized water (pH: 7.0-7.5). The effluent of each column was collected fraction wise (250 ml) for fluoride analysis. The fluoride enriched solution (pH: 7.5 ± 0.2, temperature: 30 ± 2º C) was allowed to flow down gravitationally through the fixed-bed columns.

Experimental set up for study the effect of fixed-bed depth were conducted with column of depths: 6.0, 10.0 and 14.0 cm (bed volumes, BV (L): 2.49, 4.15 and 5.82), /(bed volumes, BV (cm^3): 24.91, 41.52, 58.13),which were made by packing of 26.54, 35.8 and 44.6 g of CIHFO uniformly. The C_i employed in feed water sample was 5.0 $mg.L^{-1}$, which was fed on fixed-beds with a rate of effluent discharge 1.0 (± 0.1) ml. min^{-1} (EBCT: 24.90, 41.52 and 58.13 min).

Experiments on the effect of discharge rates of effluent (1.0, 2.0 and 3.0 $ml.min^{-1}$) (EBCT: min) using C_i of fluoride 5.0 $mg.L^{-1}$ in feed water were conducted with three separate CIHFO fixed-beds of depth 10.0 cm (BV (L): 4.15).

Experiments on the effect of fluoride concentration (Ci = 3.0, 5.0 and 9.0 $mg.L^{-1}$) in feed solution were conducted using three separate fixed-beds made by uniform packing

35.8 g CIHFO particles (bed depth: 10.0 cm, BV(L): 4.15). The solution feeding rate was fixed with a rate of effluent discharge 1.0 (± 0.1) ml.min^{-1} to move down through the fixed bed.

2.1. Water sample Collection

A mass scale water needed for column feeding was collected from a tube-well (depth: ~150ft) of college street area (Kolkata, India) was analysed for some parameters of water quality pH (7.05), iron (total) (2.89 mg.L^{-1}), calcium (55.98 mg L^{-1}), magnesium (33.69 mg.L^{-1}), hardness (89.67 mg.L^{-1}), TDS (1024 mg.L^{-1}), salinity (543 mg.L^{-1}), conductivity (769 µS) and turbidity (58 NTU) and fluoride (0.64 mg.L^{-1}). The analytical data of this water sample showed that the fluoride concentration was well below its maximum allowed level (0.64 mg. L^{-1}). Collected water sample spiked with definite volume of the standard fluoride solution to achieve the desired initial concentrations of fluoride (C_i = 3.0, 5.0 and 9.0 mg.L^{-1}) as required, which were used to evaluate performance efficacy of columns packed with CIHFO for fluoride removal.

3. Theory Applicable for Batch Study

3.1. Kinetics studies

Adsorption of any pollutant by any adsorbent is time dependant. Physico-chemical nature of adsorbent also influences the overall adsorption process. Kinetics modelling for batch adsorption process is considered very crucial aspect as it helps to determine the adsorption mechanism and also help in explore to rate determining step of ongoing adsorption process. In present batch study, Pseudo-first order, Pseudo-second order, Mass transfer, Intra-particle diffusion, Elovich Model and Richenberg model applied to study different kinetics parameters.

3.1.1. Pseudo –first order Model

The non-linear form of the pseudo-first-order kinetic model equation can be expressed as follows:

$$Q_t = Q_e\{1 - exp(-k_1.t)\} \quad \text{(Eq. 5)}$$

Where Q_e and Q_t are the amounts of pollutant adsorbed per unit weight of adsorbent (mg.g^{-1}), i.e. uptake capacity at equilibrium and at time t (min), respectively and k_1 stands for equilibrium rate constant(Biswas et al., 2009; Ghosh et al., 2014; Mukhopadhyay et al., 2017).

3.1.2. Pseudo-second order Model

The non-linear expression of Pseudo-second order kinetic Model can be expressed as follows:

$$Q_t = \frac{(t.k_2.Q_e^2)}{\{1+(t.k_2.Q_e)\}} \quad \text{(Eq. 6)}$$

Here, k_2 stands for equilibrium rate constant for Pseudo-second order kinetic Model(Biswas et al., 2009; Ghosh et al., 2014; Mukhopadhyay et al., 2017).

3.1.3. Mass Transfer

Extent of removal of any pollutant by adsorption process highly influenced by wide range of contaminants transfer from bulk solution to the surface of the solid adsorbent and at the interface of particular adsorbent or at the interface of liquid and solid

particles. For the present studies this probability was examined by using Mckay et al. model(Sharma and Weng, 2007; Singh et al., 2016a, 2016b).

$$\ln\left(\frac{C_t}{C_i} - \frac{1}{1+mk}\right) = \ln\left(\frac{mk}{1+mk}\right) - \left(\frac{1+mk}{mk}\right)\beta_1 S_s\, t \qquad \text{(Eq. 7)}$$

Here C_i and C_t signify the initial concentration of fluoride ($mg.L^{-1}$) and concentration after time t (min), respectively. The m denotes adsorbent mass per unit volume ($g.L^{-1}$), k is the Langmuir constant and S_s is the specific surface area of adsorbent per unit volume of the reaction mixture (cm^{-1}). β_1 stands for the coefficient of external mass transfer ($cm^2\ s^{-1}$). Values of β_l, the coefficient of mass transfer, were calculated at different values of temperature by the slopes and intercepts of the plots of 'ln $[C_t/C_i - 1/(1 + mk)]$ versus t'.

General mechanism thought to be involved in mass transfer is;

I. Gentle movement of pollutant from bulk solution to the upper boundary of adsorbent.
II. Slowly diffusion of adsorbate from boundary film layer to the surface of adsorbent.
III. Adhesion of adsorbate into the internal pore and spaces in between of active sites of adsorbent.
IV. Simultaneous adsorption and desorption of the adsorbate at the active sites of the adsorbent surface.

From above points it can be said that in first step, adsorption might occur in hydro-dynamic conditions that obstruct the concentration gradient in between the solution and boundary film. So, from this point of view, it cannot be a rate limiting step. Hence, external diffusion (step-2) or intra-particle diffusion, will be the slowest step that may be considered as the rate controlling step of proposed adsorption process(Mohan et al., 2016).

3.1.4. Intra-particle Diffusion Model

In an ongoing adsorption process, there is an always fair chance of diffusion of adsorbate into the pores of adsorbent which is often considered as rate controlling step of the particular adsorption process. The intraparticle diffusion rate constant (k_{id}) at different concentrations and in temperatures can be determined by the Weber–Morris model (Biswas et al., 2009; Ranjan et al., 2009)that can be expressed as follows:

$$Q_t = K_{id} t^{0.5} + C \qquad \text{(Eq. 8)}$$

where Q_t is the quantity of adsorbate ($mg.g^{-1}$) adsorbed at time t (min), K_{id} is the initial rate of intra particular diffusion calculated by the slope of the plot of Q_t *vs*.$t^{0.5}$ ($mg.L^{-1}.min^{-0.5}$) and C, is the y-intercept which gives proper information all about the boundary layer thickness(Banerjee and Chattopadhyaya, 2017). This observation was further proved by the value of the intraparticle diffusion coefficient (D), which can be calculated by the following equation.

$$D = \frac{0.03r^2}{t^{0.5}} \qquad \text{(Eq. 9)}$$

Where r (cm) stands for the average radius of the adsorbent particle and $t^{0.5}$ (min) is the time required for half of the adsorption(Biswas et al., 2009; Mohan et al., 2016).

3.1.5. Elovich Model

This equation is more familiar to determine chemisorption kinetics of any gases on heterogeneous surface of any adsorbent. Presently, this equation has been widely applied to evaluate adsorption nature of any adsorbate from aqueous medium. The equation mentioned as follows:

$$\frac{dQ_t}{dt} = a\ exp\ (abQ_t) \qquad \text{(Eq.10)}$$

Where, a signifies the rate of chemisorption at zero coverage (mg/(g/min)) and b is implies the extent of surface occupancy and activation energy required for chemisorption (g/mg). These are obtained from the slope and intercept of the plots of Q_t *vs.* ln (t) (min).

$$Q_t = \frac{1}{b}\, ln(ab) + \frac{1}{b}\, ln\left(1 + \frac{1}{ab}\right) \quad \text{(Eq. 11)}$$

This equation is the integrated form of Eq. 10 with an assumption that $Q_t = 0$, $t = 0$ as the lower of limit of integration. If value of t is much higher, i.e. $t > 1/ab$, the plots of Q_t vs. ln (t) should be linear(Ranjan et al., 2009).

3.1.6. Richenberg Model

The Richenberg expression can be used to distinguish between the film diffusion and the intra-particle diffusion, which can be given by the following equation:

$$G = 1 - \frac{6}{\Pi^2}\, exp(-\beta_t) \quad \text{(Eq. 12)}$$

Where $G = Q_t/Q_e$ and β_t is the mathematical function of G, which can be calculated from respective value of G by the following equation:

$$\beta_t = -0.4977 - ln\left(1 - \frac{Q_t}{Q_e}\right) \quad \text{(Eq. 13)}$$

The β_t values at different contact times (t) can be calculated using above equation (Eq. 13). The calculated β_t values were plotted against time t (min), and the slope was used for the calculation of factor β_t. The effective diffusion coefficient D_i ($cm^2\ s^{-1}$) has been calculated using the value of factor β_t from following equation.

$$\beta_t = \frac{\Pi D_i}{r^2} \quad \text{(Eq. 14)}$$

Where adsorbent particles were assumed to be spherical and r is assumed as the radius of the adsorbent particles. The obtained values of D_i will be thus useful to decide the process whether it is intraparticle diffusion or external diffusion. If plots are straight lines passing through the origin, then the adsorption process is governed by particle diffusion mechanisms otherwise, both external diffusion and intraparticle diffusion jointly determine the rate of adsorption(Hamayun et al., 2014; Mohammadian et al., 2016; Mohan et al., 2016; Singh et al., 2017). Values of film diffusion (D_1) and pore diffusion (D_2) also can provide information regarding the mechanism of adsorption whether it is kinetically influenced by film or pore diffusion. D_1 and D_2 can be determined by the application of following equations(Hamayun et al., 2014).

$$\frac{Q_t}{Q_e} = 6\left(\left(\frac{D_1}{\Pi a^2}\right)^{0.5}\right) t^{0.5} \quad \text{(Eq. 15)}$$

$$ln\left(1 - \frac{Q_t}{Q_e}\right) = ln\frac{6}{\Pi^2} - \left(\frac{D_2\ \Pi^2}{a^2}\ t\right) \quad \text{(Eq. 16)}$$

D_1 is calculated from the slope of the plot of Q_t/Q_e vs. $t^{0.5}$ and D_2 is calculated from the plots of ln $(1\text{-}Q_t/Q_e)$ vs. t for fluoride adsorption on GO incorporated CIHFO(Hamayun et al., 2014).

3.2. Isotherm Study

Isotherm modelling of any adsorption process is an essential step to determine the distribution pattern of any adsorbate in between solid and liquid phase at equilibrium. Hence to establish the adsorption efficiency of newly developed adsorbent, optimisation of a particular adsorption study with appropriate isotherm model is considered as basic requirement for commercialization of prepared adsorbate. To achieve the goal of present study, three isotherm models were applied namely; Langmuir, Freundlich and Dubinin - Radushkevich (D-R) isotherms. Langmuir and Freundlich are two basic fundamental isotherm model most widely applied to evaluate equilibrium data of any adsorption process. Meanwhile, D-R isotherm envisaged the nature of adsorption process.

3.2.1. Langmuir Isotherm

According to Langmuir model, each adsorbate molecule retains same adsorption energy. All active sites pose equal attraction towards adsorbate and there is no internal interaction in between molecules, hence this isotherm denotes homogeneous adsorption process. Non-linear form of Langmuir isotherm expressed as follows:

$$Q_e = \frac{Q_m K_l C_e}{[1+K_L C_e]} \quad \text{(Eq. 17)}$$

Where C_e ($mg.L^{-1}$)and Q_e ($mg.g^{-1}$) are the equilibrium fluoride concentration and equilibrium adsorption capacity. The Q_m ($mg.g^{-1}$) is the maximum monolayer adsorption capacity ($mg.g^{-1}$) and K_L (L mg^{-1}) the equilibrium constant related to net enthalpy change of the reaction(Biswas et al., 2009; Ghosh et al., 2014; Mukhopadhyay et al., 2017).

3.2.2. Freundlich Isotherm

Freundlich model assumes the non-ideal multilayer adsorption that generally associated with heterogeneous surface of adsorption sites. The non-linear expression of Freundlich can be set as,

$$Q_e = K_F \times C_e^{1/n} \quad \text{(Eq. 18)}$$

Where, the K_F is the Freundlich adsorption capacity and 1/n is an empirical constant related to the adsorption intensity(Mukhopadhyay et al., 2017)

3.2.3. Dubinin - Radushkevich (D-R) isotherm

Dubinin-Redushkevich (D–R) isotherm was elucidated to estimate the free energy of reaction and can be obtained from the equilibrium isotherm data to predict the nature of adsorption. Linear form of this isotherm is written as:

$$lnQ_e = lnQ_m - \beta E^2 \quad \text{(Eq. 19)}$$

Where E the Polanyi potential is can be extracted from the equation (17) below,

$$E = RT\ ln\left(1 + \frac{1}{C_e}\right) \quad \text{(Eq. 20)}$$

The plots of the ln Q_e against E^2 become a straight line and the values of slope and intercept of the plot was used to calculate the value of β and Q_m. Q_e and Q_m are equilibrium and maximum D-R adsorption capacities in (mol. kg^{-1}), respectively, and β is signifying activity coefficient mainly related with the mean free energy (E_{DR}) of reaction as per the following equation:

$$E_{DR} = 1/(-2\beta)^{1/2} \quad \text{(Eq. 21)}$$

Depending on the obtained value of E, the nature of adsorption (physisorption, ion-exchange or chemisorption) can be determined(Mohan et al., 2016; Mukhopadhyay et al., 2017).

3.3. Thermodynamics Studies

Study of different thermodynamic parameters such as standard free energy (ΔG^0), standard enthalpy (ΔH^0) and standard entropy (ΔS^0) changes used for evaluate thermodynamic feasibility of the adsorption process and implication of Gibb's free energy change associated with reaction process. These parameters generally calculated as per following equations:

$$\Delta G° = \Delta H° - T\Delta S° \quad \text{(Eq. 22)}$$

$$\Delta G° = -2.303RT\ log K_c \quad \text{(Eq.23)}$$

From equations (22) and (23), equation (24) could be arrived,

$$\log K_c = \frac{\Delta S°}{2.303R} - \left(\frac{\Delta H°}{2.303R}\right)\frac{1}{T} \quad \text{(Eq.24)}$$

Where, $\boldsymbol{K_c = \frac{Q_e}{C_e}}$ (Eq.25)

Q_e (mg.L^{-1}) represents equilibrium adsorbate concentration, C_e is concentration of adsorbate in bulk solution in equilibrium (mg.L^{-1})(Mohan et al., 2016; Mukhopadhyay et al., 2017).

3.4. Activation Energy

Activation energy of any kind of reaction and can be expressed by Arrhenius equation and can be expressed as

$$k_2 = A \exp (-E_a / RT) \quad \text{(Eq.26)}$$

Here, K_2 is meant as the rate constant of pseud-second order kinetic model (g mg^{-1}min^{-1}), A (g mg^{-1}min^{-1}), is a temperature independent factor and E_a (KJ mol^{-1}) is the activation energy of any particular reaction. R and T are well known and mentioned earlier. Logarithm of above equation can be demonstrated by a linear relationship of Arrhenius equation and can be represented as below.

$$\ln k_2 = \ln A + (-E_a/R)1/T \quad \text{(Eq.27)}$$